AD-A104 806 NAVAL RESEARCH LAB WASHINGTON DC F/G 20/5
COHERENT AND INCOHERENT RADIATION FROM FREE ELECTRON LASERS WIT--ETC(U)
OCT 81 H P FREUND, P SPRANGLE, D DILLENBURG
UNCLASSIFIED NRL-MR-4643 NL

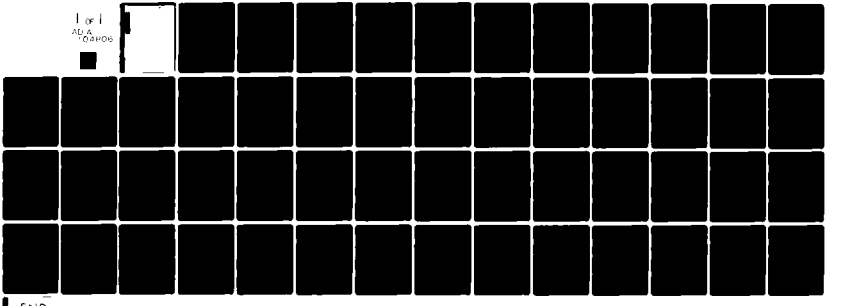

END
DATE FILMED
10-81
DTIC

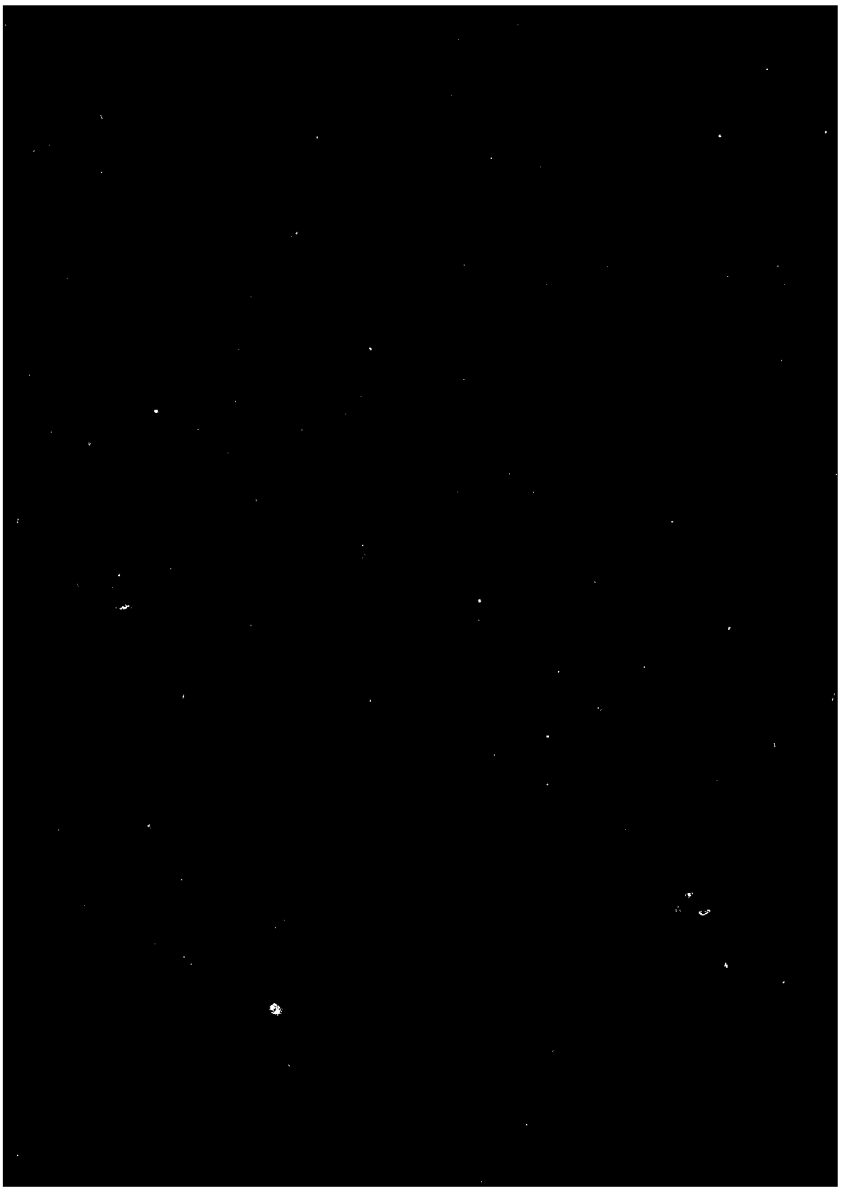

SECURITY CLASSIFICATION OF THIS PAGE (When Data Entered)

REPORT DOCUMENTATION PAGE

READ INSTRUCTIONS BEFORE COMPLETING FORM

1. REPORT NUMBER: NRL Memorandum Report 4643
2. GOVT ACCESSION NO.: AD-A104 806
3. RECIPIENT'S CATALOG NUMBER:

4. TITLE (and Subtitle): COHERENT AND INCOHERENT RADIATION FROM FREE ELECTRON LASERS WITH AN AXIAL GUIDE FIELD
5. TYPE OF REPORT & PERIOD COVERED: Interim report on a continuing NRL problem.
6. PERFORMING ORG. REPORT NUMBER:

7. AUTHOR(s): H. P. Freund*, P. Sprangle, D. Dillenburg**, E. H. da Jornada**, B. Liberman**, and R. S. Schneider**
8. CONTRACT OR GRANT NUMBER(s):

9. PERFORMING ORGANIZATION NAME AND ADDRESS: Naval Research Laboratory, Washington, DC 20375
10. PROGRAM ELEMENT, PROJECT, TASK AREA & WORK UNIT NUMBERS: 62332N; WF-32-389-592; 47-0920-0-1

11. CONTROLLING OFFICE NAME AND ADDRESS: Naval Air Systems Command, Washington, DC 20360
12. REPORT DATE: October 1981
13. NUMBER OF PAGES: 53

14. MONITORING AGENCY NAME & ADDRESS (if different from Controlling Office):
15. SECURITY CLASS. (of this report): UNCLASSIFIED
15a. DECLASSIFICATION/DOWNGRADING SCHEDULE:

16. DISTRIBUTION STATEMENT (of this Report)

Approved for public release; distribution unlimited.

17. DISTRIBUTION STATEMENT (of the abstract entered in Block 20, if different from Report)

18. SUPPLEMENTARY NOTES

*Present address: Science Applications, Inc., McLean, VA 22102
**Present address: Instituto de Fisica, Universidade Federal do Rio Grande do Sul, 90.000 Porto Alegre-RS, Brazil

19. KEY WORDS (Continue on reverse side if necessary and identify by block number)

Microwave radiation
Free electron laser
Relativistic high power radiation source

20. ABSTRACT (Continue on reverse side if necessary and identify by block number)

The spontaneous and induced emission from a free electron laser is treated for the case in which an axial magnetic field is imposed in addition to the helical, axially periodic wiggler magnetic field. The classes of possible single-particle trajectories in this configuration are discussed, and the results are applied to a calculation of the incoherent radiation from a beam of relativistic electrons in the system. The coherent radiation is treated by solving the Vlasov-Maxwell equations for the linear gain in the tenuous beam limit, where the beam plasma frequency is much less than the radiation frequency and self-field effects can be ignored.

DD FORM 1 JAN 73 1473 EDITION OF 1 NOV 65 IS OBSOLETE
S/N 0102-014-6601

SECURITY CLASSIFICATION OF THIS PAGE (When Data Entered)

9517

CONTENTS

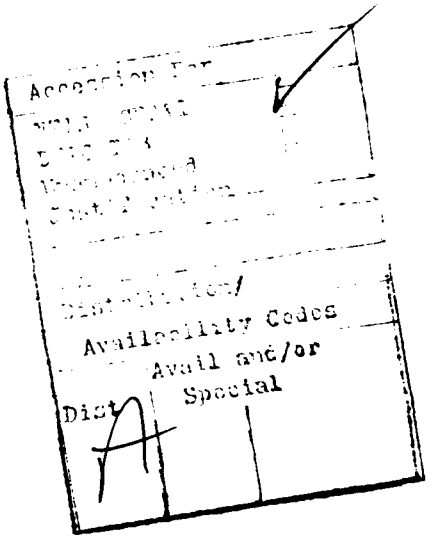

COHERENT AND INCOHERENT RADIATION FROM FREE ELECTRON LASERS WITH AN AXIAL GUIDE FIELD

I. INTRODUCTION

Recent experiments[1-3] have amply demonstrated the usefulness of the free electron laser as a tunable source of coherent submillimeter radiation, and have stimulated interest in a variety of experimental configurations. Theoretical work[4-6] in this regard has concentrated on the case in which a relatively low density (i.e., self-field effects are negligible) relativistic electron beam is propagated through a periodic helically symmetric magnetic field, referred to as the "wiggler" field. In the beam frame the wiggler field appears as a backwards propagating electromagnetic wave, and radiation is produced by means of coherent scattering of this wave off electromagnetic fluctuations in the beam. Another configuration employed is one in which an axial guide field is present, and is used principally, but not exclusively, in the regime in which electron densities and currents are sufficiently high that the axial field is required to contain the beam against the effects of the self-fields. Theoretical analyses of the coherent radiation mechanism in this regime have begun to appear in the literature for this configuration as well.[7-11]

It is our purpose in this work to treat both the coherent and incoherent radiation from a free electron laser configuration which contains an axial guide field, in the low density limit. Full relativistic effects are included, but the self-fields of the beam are neglected. The principal application of this study to existing experiments is the Stanford University free electron laser[1,2] in which a low current ($\sim$ 2 A), high energy (24-43 MeV) beam was injected into a drift tube in which

Manuscript submitted August 25, 1981.

an axial guide field of 1 kG and a wiggler field of about 2.4 kG were applied. In this regime collective beam effects are negligible.

The organization of the paper is as follows. In Sec. II, we discuss the single-particle trajectories of electrons in a magnetic field geometry composed of a combined axial guide field and helical wiggler field. The incoherent, spontaneous emission spectrum is calculated in Sec. III using test particle techniques, and the linear gain is found in Sec. IV in the limit of a low density beam. In treating a low density beam, we restrict the analysis of the linear gain to the small-signal regime but provide a fully kinetic derivation of the gain based upon the Vlasov-Maxwell equations. This is in contrast to the work of Kwan and Dawson[7] and Bernstein and Friedland[10] in which collective effects due to high beam density were included in the context of a fluid theory of the interaction. The small-signal gain has also been considered by Friedland and Hirschfield[11] by means of a fluid analysis. Thus, we provide a fully kinetic expression for the small-signal gain and an extensive description of the parametric dependence of the gain in the cold beam limit. A summary and discussion is given in Sec. V.

II. SINGLE-PARTICLE TRAJECTORIES

The wiggler field is generally due to a helical current winding and the resultant field can be shown, in a self-consistent way, to be of the form[12,13]

$$\underset{\sim}{B} = B_0 \hat{\underset{\sim}{e}}_z + \underset{\sim}{B}_w(r,z), \tag{1}$$

where the wiggler field is derived from a vector potential of the form

$$\underset{\sim}{A}_w = -\frac{2B_w}{k_w}\left(\frac{1}{k_w r} I_1(k_w r)\cos(\theta - k_w z)\,\hat{\underset{\sim}{e}}_r - I_1'(k_w r)\sin(\theta - k_w z)\,\hat{\underset{\sim}{e}}_\theta\right), \tag{2}$$

in cylindrical coordinates. In Eq. (2), B_w and k_w ($\equiv 2\pi/\lambda_w$, where λ_w is the wiggler period) are assumed to be constant, and I_1 and I_1' are the modified Bessel function of the first kind and its derivative respectively. In most free electron laser experiments, however, the initial beam radius is a small fraction of the wiggler period, and expansion in powers of $k_w r$ yields

$$\underset{\sim}{B}_w \simeq B_w\,(\hat{\underset{\sim}{e}}_x \cos k_w z + \hat{\underset{\sim}{e}}_y \sin k_w z). \tag{3}$$

Rather than work in the laboratory frame, we choose to transform to the frame rotating with the wiggler field. To this end we define $\hat{\underset{\sim}{e}}_1 = \hat{\underset{\sim}{e}}_x \cos k_w z + \hat{\underset{\sim}{e}}_y \sin k_w z$, $\hat{\underset{\sim}{e}}_2 = -\hat{\underset{\sim}{e}}_x \sin k_w z + \hat{\underset{\sim}{e}}_y \cos k_w z$, $\hat{\underset{\sim}{e}}_3 = \hat{\underset{\sim}{e}}_z$ and write the orbit equations corresponding to the field structure given in (1) and (3) in the form

$$\dot{v}_1 = v_2 (k_w v_3 - \Omega_0),$$
$$\dot{v}_2 = - \Omega_w v_3 - v_1 (k_w v_3 - \Omega_0), \tag{4}$$
$$\dot{v}_3 = \Omega_w v_2,$$

where $\Omega_0 \equiv |eB_0/\gamma mc|$, $\Omega_w \equiv |eB_w/\gamma mc|$, and $\gamma \equiv (1 - v^2/c^2)^{-\frac{1}{2}}$. Since the total energy is a conserved quantity $v^2 \equiv v_1^2 + v_2^2 + v_3^2$ is a constant of the motion and Eqs. (4) are fully relativistic. The principal benefit derived from this transformation is that the equations of motion are now coordinate-independent, and depend only on the components of the velocity and their derivatives.

In addition to the total energy, a second constant of the motion can be found by elimination of v_2 from (4); specifically, $u \equiv v_1 - k_w \times (v_3 - \Omega_0/k_w)^2/2\Omega_w$. This is analogous to the axial invariant discussed by Davidson and Uhm,[14] which in the $B_w \to 0$ limit implies that the axial velocity is conserved and defines the rotating frame to be that of the Larmor rotation of an electron in a uniform magnetic field. By means of these constants, the problem can be reduced to the solution of a single nonlinear differential equation for v_3,

$$(dx/d\tau)^2 + \Phi(x) = 0, \tag{5}$$

where $x \equiv \beta_3 - \beta_0$, $\tau \equiv \Omega_0 t/2$, $\beta_3 \equiv v_3/c$, $\beta_0 \equiv \Omega_0/k_w c$,

$$\Phi(x) \equiv x^4 + 4\epsilon\beta_0(\epsilon\beta_0 + \beta_u)\, x^2 + 8\epsilon^2\beta_0^3 x + 4\epsilon^2\beta_0^2(\beta_0^2 + \beta_u^2 - \beta_v^2),$$

$\epsilon \equiv B_w/B_0$, $\beta_v \equiv v/c$, and $\beta_u \equiv u/c$. Note that Eq. (5) has the trivial solution $x = 0$ (i.e., v_3 = constant) in the limit of a uniform axial magnetic field ($B_w \to 0$).

A detailed discussion of the solutions of Eq. (5) has been given by Freund and Drobot;[15] however, we restrict our attention here to solutions

corresponding to relatively uniform axial velocities. The reason for this is that the radiation mechanism is a resonant one in which the emission frequency is given by $\omega \simeq 2\gamma_z^2 k_w v_3$, where $\gamma_z = (1 - v_3^2/c^2)^{-\frac{1}{2}}$. As a result, variations in the axial velocity of the order of Δv_3 lead to a broadening of the emission spectrum which scales as $\Delta\omega \sim 2\gamma_z^3 k_w \Delta v_3$. Thus, while small oscillations in v_3 about some bulk axial velocity lead to a relatively narrow bandwidth, large oscillations can result in spectral broadening with a corresponding decrease in the linear gain.

The conditions which lead to small oscillations in the axial velocity can be investigated by consideration of the roots of the pseudopotential $\Phi(x)$. Physically meaningful (i.e., real) solutions are possible only when $\Phi < 0$; therefore, the real roots of the pseudopotential correspond to the bounds on the oscillation about some bulk axial velocity (defined by the local minimum in Φ between the roots). The typical character of the pseudopotential when $\varepsilon < 1$ and $\beta_0 > 1$ is shown in Fig. 1. In this regime, the pseudopotential has two real roots which for given values of ε, β_0, and v shift in both position and spacing with variations in β_u within some fixed range. The extrema in the range of β_u occur when the real roots of Φ are degenerate, and correspond to solutions with constant axial velocity[15,16]

$$\begin{aligned} v_1 &= -\frac{\Omega_w v_{||}}{k_w v_{||} - \Omega_0}, \\ v_2 &= 0, \\ v_3 &= v_{||}, \end{aligned} \tag{6}$$

where the axial velocity $v_{||}$ is given by $v^2 = v_1^2 + v_3^2$ for some choice of the total energy.

The values of β_3 (= $\beta_0 + x$) corresponding to the real roots of Φ are shown in Fig. 2 versus β_u for $\varepsilon = .1$ and $\beta_0 = 1$, and 4. Thus, the figure describes the bounds on the oscillations in the axial velocity for given β_u. It is important to recognize that small deviations in β_u from the extrema result in trajectories which do not differ greatly from those with uniform axial velocities. Because of this two electrons which are characterized by only slightly different values of β_u and which are close together at some point will not undergo a large separation in the course of their orbits. To be more specific, an initially bunched electron beam will tend to remain bunched. This describes an "orbitally stable" uniform-v_3 solution, in the sense discussed by Friedland.[16] A quantitative test for orbital stability can be expressed in the form

$$\frac{\varepsilon^2 \beta_0^3}{\left(\frac{v_{||}}{c} - \beta_0\right)^3} < 1,$$

which (since $v_{||} < c$) is trivially satisfied for the uniform-v_3 trajectories when $\beta_0 > 1$.

In contrast, when β_0 is less than unity the pseudopotential can have as many as four real roots and as many as four uniform-v_3 orbits appear. An example of this is shown in Fig. 3, where we plot β_3 corresponding to the roots versus β_u for $\varepsilon = .1$, and $\beta_0 = .5$ and 1. The orbits with uniform axial velocity correspond to the points of vertical slope in the figure, and when $\beta_0 = .5$ four such trajectories appear. Three of these orbits

are stable; however, the trajectory corresponding to point A in the figure represents a fundamentally different class of solution than the other three. The behavior of the pseudopotential for values of β_u in the vicinity of a stable orbit is shown in Fig. 1. In contrast, the behavior of Φ with β_u in the vicinity of point A is shown in Fig. 4 in which the uniform-v_3 trajectory is obtained when the central maximum is zero. Arbitrarily small deviations from this condition result in drastically different types of trajectory with large fluctuations in the axial velocity. Such uniform-v_3 trajectories are referred to as being "orbitally unstable," since a bunched electron beam with a spread in the axial invariant in the vicinity of point A will rapidly disperse.

As β_0 decreases further, the range of β_u in which Φ possesses four real roots increases, as shown in Fig. 5 for $\beta_0 = .1$. In particular, the high axial velocity, uniform-v_3 trajectory for motion parallel to $\underset{\sim}{B}_0$ becomes more pronounced as β_0 decreases further relative to ε. This characteristic of the solutions in the small-β_0 regime exists even where $\varepsilon > 1$ (see Fig. 6). Finally, we conclude that the requirement that electrons propagate with relatively small fluctuations in axial velocity is most difficult to satisfy when $\beta_0 \sim 1$. The natural corollary, therefore, that extremely broadbanded emission will occur in this regime, is supported by observation.[17,18]

In order to treat cases of nearly uniform axial velocity we implicitly restrict consideration to trajectories corresponding to the stable uniform-v_3 solutions. In this limit, we can write approximate solutions for the momenta in the laboratory frame as

$$p_x = \frac{\Omega_w p_\parallel}{\Omega_0 - k_w v_\parallel} \cos k_w z + P_x \cos \Omega_0 t - P_y \sin \Omega_0 t,$$

$$p_y = \frac{\Omega_w p_\parallel}{\Omega_0 - k_w v_\parallel} \sin k_w z + P_x \sin \Omega_0 t + P_y \cos \Omega_0 t, \qquad (7)$$

$$p_z = p_\parallel - \frac{\Omega_w}{\Omega_0 - k_w v_\parallel} \left[P_x \cos (k_w z - \Omega_0 t) - P_y \sin (k_w z - \Omega_0 t)\right]$$

where $p_\parallel$, P_x and P_y are approximate constants of the motion, and $v_\parallel \equiv p_\parallel / \gamma m$. Observe that in the limit of a vanishing axial guide field Eqs. (7) recover the well-known result in which P_x and P_y are the canonical momenta in the transverse direction. This approximation remains valid as long as $P_x^2 + P_y^2 \ll p_\parallel^2$, and the total momentum is given by

$$p^2 = P_x^2 + P_y^2 + \left(1 + \frac{\Omega_w^2}{(\Omega_0 - k_w v_\parallel)^2}\right) p_\parallel^2 \qquad (8)$$

to within terms of order ε^2. The form of these trajectories is shown schematically in Fig. 7. Particle motion predominantly follows the helical wiggler, but also contains a small component of Larmor procession due to the axial field.

III. SPONTANEOUS EMISSION

The time-averaged radiated power P can be computed by means of the equation

$$P = -\lim_{T\to\infty} \frac{1}{T} \int_{-T/2}^{T/2} dt \int d^3x \; \underset{\sim}{E}(\underset{\sim}{x},t) \cdot \underset{\sim}{J}(\underset{\sim}{x},t), \tag{9}$$

where $\underset{\sim}{E}(\underset{\sim}{x},t)$ denotes the microscopic radiation field, and

$$\underset{\sim}{J}(\underset{\sim}{x},t) = -e \sum_{j=1}^{N_b} \underset{\sim}{v}_j(t) \; \delta(\underset{\sim}{x} - \underset{\sim}{x}_j(t)) \tag{10}$$

is the source current composed of the sum of the microscopic currents due to all N_b electrons in the beam during the interaction time $-T/2 < t < T/2$. The radiated power can be expressed in terms of the Fourier amplitudes of the microscopic fields and source currents in the following manner

$$P = -2(2\pi)^4 \lim_{T\to\infty} \frac{1}{T} \int d^3k \int_0^\infty d\omega \; \mathrm{Re}\,(\underset{\sim}{E}_{\underset{\sim}{k},\omega} \cdot \underset{\sim}{J}^*_{\underset{\sim}{k},\omega}), \tag{11}$$

where the asterisk (*) denotes the complex conjugate, and the Fourier amplitude is defined as $f_{\underset{\sim}{k},\omega} = \int d^3k \int_{-\infty}^{\infty} d\omega \; \exp(i\omega t - i\underset{\sim}{k} \cdot \underset{\sim}{x}) \; f(\underset{\sim}{x},t)$. A self-consistent relation between the fields and source currents depends upon the dielectric properties of the beam, and can be written as

$$\underset{\sim}{\Lambda}_{\underset{\sim}{k},\omega} \cdot \underset{\sim}{E}_{\underset{\sim}{k},\omega} = \frac{4\pi i}{\omega} \underset{\sim}{J}_{\underset{\sim}{k},\omega}, \tag{12}$$

where the dispersion tensor

$$\underset{\sim}{\Lambda}_{\underset{\sim}{k},\omega} = (1 - n^2) \; \underset{\sim}{I} + n^2 \, \hat{\underset{\sim}{k}}\hat{\underset{\sim}{k}} + \underset{\sim}{\varepsilon}_{\underset{\sim}{k},\omega}, \tag{13}$$

$n \; (\equiv ck/\omega)$ is the index of refraction, $\underset{\sim}{I}$ is the unit dyadic,

$\hat{\underset{\sim}{k}} \equiv \underset{\sim}{k}/|\underset{\sim}{k}|$, and $\underset{\sim}{\underset{\sim}{\varepsilon}}_{\underset{\sim}{k},\omega}$ is the beam dielectric tensor. For the case of a diffuse beam, in which the radiation frequency greatly exceeds the electron plasma frequency, $\underset{\sim}{\underset{\sim}{\varepsilon}}_{\underset{\sim}{k},\omega} \simeq \underset{\sim}{\underset{\sim}{I}}$ and (12) can be inverted to give

$$\underset{\sim}{E}_{\underset{\sim}{k},\omega} = -(4\pi i\omega)/(\omega^2 - c^2k^2)\left[\underset{\sim}{J}_{\underset{\sim}{k},\omega} - n^2\hat{\underset{\sim}{k}}(\hat{\underset{\sim}{k}} \cdot \underset{\sim}{J}_{\underset{\sim}{k},\omega})\right]. \tag{14}$$

As a result, if the emissivity $\eta(\omega, \hat{\Omega}_{\underset{\sim}{k}})$ is defined to be the power radiated per unit frequency and volume into the solid angle $\hat{\Omega}_{\underset{\sim}{k}}$ subtended by $\hat{\underset{\sim}{k}}$, then we find

$$\eta(\omega, \hat{\Omega}_{\underset{\sim}{k}}) = (2\pi)^6 (\omega^2/Vc^3) \lim_{T\to\infty} \frac{1}{T} \left(|\underset{\sim}{J}_{\underset{\sim}{k},\omega}|^2 - |\hat{\underset{\sim}{k}} \cdot \underset{\sim}{J}_{\underset{\sim}{k},\omega}|^2\right)\Big|_{k = \omega/c}, \tag{15}$$

where V is the total volume of the interaction region. The radiation spectrum, therefore, can be determined from (15) with a knowledge of the single-particle orbits (7) necessary to compute the source current.

Using the trajectories in (7), we find that after transforming to the frame ($\hat{\underset{\sim}{e}}_\perp = \cos\psi\,\hat{\underset{\sim}{e}}_x + \sin\psi\,\hat{\underset{\sim}{e}}_y$, $\hat{\underset{\sim}{e}}_\psi = -\sin\psi\,\hat{\underset{\sim}{e}}_x + \cos\psi\,\hat{\underset{\sim}{e}}_y$, and $\tan\psi = k_y/k_x$) in which $\underset{\sim}{k} = k_\perp \hat{\underset{\sim}{e}}_\perp + k_z \hat{\underset{\sim}{e}}_z$ ($k = \sqrt{k_x^2 + k_y^2}$) the source current is

$$\underset{\sim}{J}_{\underset{\sim}{k},\omega} = -\frac{e}{(2\pi)^3} \lim_{T\to\infty} \sum_{j=1}^{N_b} \exp(-i\underset{\sim}{k}\cdot\underset{\sim}{x}_0^{(j)}) \sum_{\ell,m,n=-\infty}^{\infty} \underset{\sim}{V}_{\ell mn}^{(j)}$$

$$\times \frac{\sin\left[(\omega - k_z v_\parallel^{(j)} - (\ell+n)k_w v_\parallel^{(j)} - (m-n)\Omega_0^{(j)})T/2\right]}{\pi(\omega - k_z v_\parallel^{(j)} - (\ell+n)k_w v_\parallel^{(j)} - (m-n)\Omega_0^{(j)})} \exp\left[ib_\perp^{(j)}\sin(\phi^{(j)} - \psi) - im(\phi^{(j)} - \psi)\right] \tag{16}$$

$$\times \exp\left[ib^{(j)}\sin(k_w z_0^{(j)} - \psi) - i\ell(k_w z_0^{(j)} - \psi)\right] \exp\left[ib_\parallel^{(j)}\sin(k_w z_0^{(j)} - \phi^{(j)}) - in(k_w z_0^{(j)} - \phi^{(j)})\right]$$

where $\underset{\sim}{x}_0^{(j)}$ defines the initial position of the j^{th} electron, $\phi^{(j)} \equiv \tan^{-1}(P_y/P_x)$, $b^{(j)} \equiv k_\perp \Omega_w^{(j)}/k_w(\Omega_0^{(j)}-k_w v_{||}^{(j)})$, $b_\perp^{(j)} \equiv k_\perp V_\perp^{(j)}/\Omega_0^{(j)}$, $b_z^{(j)} \equiv k_z V_\perp^{(j)} \Omega_w^{(j)}/(\Omega_0^{(j)}-k_w v_{||}^{(j)})^2$, and $V_\perp^2 \equiv (P_x^2 + P_y^2)/\gamma m$. In addition,

$$\underset{\sim}{V}_{\ell mn}^{(j)} = J_n(b_z^{(j)})\left[\left(\frac{\ell k_w v^{(j)}+m\Omega_0^{(j)}}{k_\perp}\right) J_\ell(b^{(j)})J_m(b_\perp^{(j)})\hat{\underset{\sim}{\epsilon}}_\perp \right.$$

$$+ i\left(v_w^{(j)} J_\ell'(b^{(j)})J_m(b_\perp^{(j)}) + V_\perp^{(j)} J_\ell(b^{(j)})J_m'(b_\perp^{(j)})\right)\hat{\underset{\sim}{\epsilon}}_\psi$$

$$\left. + \left(v_{||}^{(j)} - \frac{n(\Omega_0^{(j)}-k_w v_{||}^{(j)})}{k_\perp}\right) J_\ell(b^{(j)})J_m(b_\perp^{(j)})\hat{\underset{\sim}{\epsilon}}_z\right] , \tag{17}$$

where $v_w \equiv \Omega_w v_{||}/(\Omega_0-k_w v_{||})$, and J_p and J_p' are the regular Bessel function of the first kind and its derivative respectively. In computing the quadratic forms of the source current which appear in the emissivity (15), we impose a random phase approximation to obtain

$$\eta(\omega,\underset{\sim}{\Omega}_{\underset{\sim}{k}}) = \frac{e^2\omega^2}{2\pi c^3 V} \sum_{j=1}^{N_b} \sum_{\ell,m,n=-\infty}^{\infty} \sum_{\ell',m',n'=-\infty}^{\infty} \delta_{\ell+n,\ell'+n}\ \delta_{m-n,m'-n'}$$

$$\times \left(\underset{\sim}{V}_{\ell mn}^{(j)} \cdot \underset{\sim}{V}_{\ell' m' n'}^{(j)*} - \hat{\underset{\sim}{k}} \cdot \underset{\sim}{V}_{\ell mn}^{(j)} \hat{\underset{\sim}{k}} \cdot \underset{\sim}{V}_{\ell' m' n'}^{(j)*}\right) \delta(\omega-k_z v_{||}^{(j)} - (\ell+n)k_w v_{||}^{(j)} - (m-n)\Omega_0^{(j)})\Big|_{k=\omega/c} \tag{18}$$

We treat the emissivity in the limit in which $b_z^{(j)} << 1$, which is generally valid as long as $2\gamma^2 \varepsilon \beta_0 (V_\perp/v_{||}) << 1$. When this condition is satisfied the dominant terms in (18) are those for which $n = n' = 0$, and the emissivity takes on the relatively simple form

$$\eta(\omega,\underset{\sim}{\Omega}_k) \simeq \frac{e^2\omega^2}{2\pi c^3 V}\sum_{j=1}^{N_b}\sum_{\ell,m=-\infty}^{\infty}\left\{\left[\left(\frac{\ell k_w v_{\|}^{(j)}+m\Omega_0^{(j)}}{k_\perp}\right)\cos\theta - v_{\|}^{(j)}\sin\theta\right]^2 J_\ell^2(b^{(j)})J_m^2(b_\perp^{(j)})\right.$$

$$\left. + \left[v_w^{(j)}J_\ell'(b^{(j)})J_m(b_\perp^{(j)}) + V_\perp^{(j)}J_\ell(b^{(j)})J_m'(b_\perp^{(j)})\right]^2\right\} \tag{19}$$

$$\times\ \delta(\omega - k_z v_{\|}^{(j)} - \ell k_w v_{\|}^{(j)} - m\Omega_0^{(j)})\Big|_{k=\omega/c},$$

where $\theta \equiv \cos^{-1}(\hat{\underset{\sim}{k}}\cdot\hat{\underset{\sim}{e}}_z)$ is the polar angle between the wave vector and the axial guide field.

We now convert the discrete sum over individual electrons in (18) and (19) into a continuous integral over the beam distribution function by making the replacement $V^{-1}\sum_{j=1}^{N_b} \rightarrow n_b\int dP_x dP_y dp F_b$, where $n_b \equiv N_b/V$ and the beam distribution F_b is assumed to be a function of (P_x,P_y,p). As a consequence,

$$\eta(\omega,\underset{\sim}{\Omega}_k) \simeq \frac{e^2 n_b \omega^2}{2\pi c^3}\int dP_x dP_y dp F_b \sum_{\ell,m=-\infty}^{\infty}\left\{\left[\left(\frac{\ell k_w v_{\|}+m\Omega_0}{k_\perp}\right)\cos\theta - v_{\|}\sin\theta\right]^2 J_\ell^2(b)J_m^2(b_\perp)\right.$$

$$\left. + \left[v_w J_\ell'(b)J_m(b_\perp) + V_\perp J_\ell(b)J_m'(b_\perp)\right]^2\right\}$$

$$\times\ \delta(\omega - k_z v_{\|} - \ell k_w v_{\|} - m\Omega_0)\Big|_{k=\omega/c}, \tag{20}$$

where $v_{\|}$ is determined by means of Eq. (8). Since (8) is, in general,

a quartic polynomial for $v_{||}$, care must be exercised in selecting the appropriate root. In the limit of propagation parallel to the axial guide field, (20) reduces to the comparatively simple form

$$\eta(\omega,\Omega_{\underset{\sim}{k}=\hat{e}_z}) \simeq \frac{e^2 n_b \omega^2}{2\pi c} \int dP_x dP_y dp F_b \left\{ \frac{v_w^2}{c^2} \delta(\omega-(k+k_w)v_{||}) + \frac{v_\perp^2}{c^2} \delta(\omega-kv_{||}-\Omega_0) \right\}_{k=\omega/c} . \tag{21}$$

Thus, the incoherent radiation corresponding to the usual free electron laser resonance at $\omega \sim 2\gamma_z^2 k_w v_{||}$ scales as v_w^2. The emission at the cyclotron resonance is expected to be much less intense in this regime in which it is required that $V_\perp^2 < v_w^2$ in the derivation of the relativistic trajectories (7). An important consequence of this analysis is that the emissivity in the presence of an axial guide field is enhanced by a factor of $(\Omega_0/k_w v_{||} - 1)^{-2}$. Note, however, that there is no singularity since $v_{||}$ must be computed from $v_{||}^2 + v_w^2 = v^2 \leq c^2$.

In order to illustrate typical noise levels and spectra to be expected in the course of operation of a free electron laser we assume a distribution of the form $F(P_x,P_y,p) = n_b \delta(P_x)\delta(P_y)G_b(p)$, and model the variation in total momentum with a distribution of the form

$$G_b(p) = \frac{\Delta p}{\pi} \frac{1}{(p-p_0)^2 + \Delta p^2} ,$$

where p_0 characterizes the bulk momentum in the beam and Δp describes the momentum spread. Note that since $P_x = P_y = 0$ the component of the motion

describing Larmor rotation is assumed to be negligible, and the noise spectrum is predominantly associated with the free electron laser resonance. As a consequence, the emissivity is of the form

$$\eta(\omega,\Omega_{\hat{k}=\hat{e}_z}) \simeq \frac{\Omega_w^2}{8\pi^3 k_w^2}\frac{m\omega_b^2}{c^3}\frac{\omega^4}{(\omega+k_w c)^3}\frac{(1+u_{ph}^2)^{3/2}}{(\beta_0\gamma_0-u_{ph})^2}\frac{\Delta u}{(u_{ph}-u_0)^2+\Delta u^2}, \quad (22)$$

where $\omega_b^2 \equiv 4\pi e^2 n_b/m$, $\Delta u \equiv \Delta p/mc$, $u_0 \equiv p_0/mc$, and

$$u_{ph} = \frac{\omega}{k_w c}\sqrt{\frac{1+\Omega_w^2/k_w^2c^2}{1+2\omega/k_w c}}.$$

As an example, we shall evaluate the emissivity (22) for a 1 Amp electron beam characterized by a bulk energy of 1.4 MeV with a 3% energy spread and a 3 cm beam radius. The beam density, therefore, is approximately $n_b \simeq 1 \times 10^9$ cm^{-3}. In addition, we shall assume the wiggler amplitude and period to be 700 G and 3 cm respectively, and the axial guide field to be 15 kG. The resulting noise spectrum is shown in Fig. 8. The peak intensity is of the order of .013 pW-Hz^{-1}-cm^{-3} and occurs at a frequency of approximately 240 GHz with a half-width of 6%.

IV. COHERENT EMISSION

In this section we derive the linearized gain by solution of the Vlasov-Maxwell equations. If the distribution is written as the sum of equilibrium and fluctuating components $f_b(z,\underset{\sim}{p},t) = F_b(P_x,P_y,p) + \delta f_b(z,\underset{\sim}{p},t)$, then the formal solution of the Vlasov equation for the perturbed distribution is

$$\delta f_b(z,\underset{\sim}{p},t(z)) = e\int_0^z \frac{dz'}{v_z(z')} \left(\delta\underset{\sim}{E}(z',t(z')) + \frac{1}{c}\underset{\sim}{v}(z')\times\delta\underset{\sim}{B}(z',t(z'))\right) \cdot \frac{\partial F_b}{\partial \underset{\sim}{p}(z')} \qquad (23)$$

to first order in the radiation fields, where the solution is parametrized in terms of the axial distance from the start of the interaction region (at $z = 0$), and $t(z) \equiv t_0 + \int_0^z dz'/v_z(z')$ is the sum of the time required for an electron to traverse the distance and the entry time t_0. The transverse components of the trajectory, therefore, are written in the form $p_x = p_w \cos k_w z + P_x \cos\Omega_0 t(z) - P_y \sin\Omega_0 t(z)$, and $p_y = p_w \sin k_w z + P_x \sin\Omega_0 t(z) + P_y \cos\Omega_0 t(z)$.

We assume plane wave solutions of the form $\exp(i\omega t)$ and choose to work with scalar and vector potentials of the form

$$\delta\Phi(z,t) = \frac{1}{2}\,\delta\hat{\Phi}(z)\exp(-i\omega t) + \text{c.c.},$$

and

$$\delta\underset{\sim}{A}(z,t) = \frac{1}{2}\,\delta\hat{\underset{\sim}{A}}(z)\exp(-i\omega t) + \text{c.c.},$$

where it is evident that $\hat{e}_z \cdot \delta\hat{A} = 0$. After transformation to the basis $\hat{e}_\pm = \frac{1}{2}(\hat{e}_x \pm i\hat{e}_y)$, therefore, the perturbed distribution can be written as $\delta f_b(z,p,\tau(z)) = \delta\hat{f}_b(z,p)\exp(-i\omega t(z)) + c.c.$, where

$$\delta\hat{f}_b(z,p) = \frac{e}{2c}\int_0^z dz' \frac{\exp(i\omega\tau(z,z'))}{v_z(z')}\Big\{[-cp_z(z')\partial_{z'}\delta\hat{\phi}(z')+i\omega(p_-(z')\delta\hat{A}_+(z')$$
$$+ i\omega(p_-(z')\delta\hat{A}_+(z') + p_+(z')\delta\hat{A}_-(z'))]\ \frac{1}{p}\frac{\partial}{\partial p}$$
$$+ \exp(i\Omega_0 t(z'))(i\omega - v_z(z')\partial_{z'})\delta\hat{A}_+(z')\left(\frac{\partial}{\partial P_x} + i\frac{\partial}{\partial P_y}\right)$$
$$+ \exp(-i\Omega_0 t(z'))(i\omega - v_z(z')\partial_{z'})\delta\hat{A}_-(z')\left(\frac{\partial}{\partial P_x} - i\frac{\partial}{\partial P_y}\right)\Big\}F_b \qquad (24)$$

$p_\pm \equiv p_x \mp ip_y$, $\delta\hat{A}_\pm \equiv \frac{1}{2}(\delta\hat{A}_x \mp i\delta\hat{A}_y)$, and $\tau(z,z') \equiv \int_{z'}^{z} dz''/v_z(z'')$. Using (24) the perturbed current, $\delta\underset{\sim}{J}(z,t) = (\delta\hat{J}_+(z)\hat{e}_+ + \delta J_-(z)\hat{e}_- + \delta\hat{J}_z(z)\hat{e}_z)\exp(-i\omega t)$ + c.c., can be computed as follows

$$\begin{pmatrix}\delta\hat{J}_+\\ \delta\hat{J}_-\\ \delta\hat{J}_z\end{pmatrix} = -\frac{e}{m}\int dP_x dP_y dp\ \frac{p}{p_z}\ \delta\hat{f}_b(z,p)\begin{pmatrix}p_+\\ p_-\\ p_z\end{pmatrix} \qquad (25)$$

Since the assumption of small P_x and P_y is central to the analysis, we shall adopt an equilibrium distribution of the form

$$F_b(P_x,P_y,p) = n_b\delta(P_x)\delta(P_y)G_b(p), \qquad (26)$$

in the interest of computational simplicity. Here $G_b(p)$ is an arbitrary

function of the magnitude of the momentum subject only to the normalization $\int_0^\infty dp p G_b(p)/p_z = 1$. Using (26), we find the perturbed currents

$$\delta\hat{J}_{\pm} = \frac{\omega_b^2}{8\pi c}\int_0^\infty dp\, \frac{p}{p_z\gamma} \left\{ \exp(\mp i\Omega_0\tau(z)) \left(2+\frac{p_+p_-}{p_z^2}\right) D_{\pm} + \exp(\pm i\Omega_0\tau(z)) \frac{p_\pm^2}{p_z^2} D_{\mp} \right.$$

$$\left. + p_{\pm}\left(\frac{\partial}{\partial P_x} + i\frac{\partial}{\partial P_y}\right) D_+ + p_{\pm}\left(\frac{\partial}{\partial P_x} - i\frac{\partial}{\partial P_y}\right) D_- - p_{\pm} D_z \frac{\partial}{\partial p} \right\} G_b(p), \qquad (27)$$

$$P_x=P_y=0$$

$$\delta\hat{J}_z = \frac{\omega_b^2}{8\pi c}\int_0^\infty dp\, \frac{p}{\gamma} \left\{ \left(\frac{\partial}{\partial P_x} + i\frac{\partial}{\partial P_y}\right) D_+ + \left(\frac{\partial}{\partial P_x} - i\frac{\partial}{\partial P_y}\right) D_- - D_z \frac{\partial}{\partial p} \right\} G_b(p), \qquad (28)$$

$$P_x=P_y=0$$

where $p_z = p_\parallel \equiv (p^2-p_w^2)^{1/2}$, $p_{\pm} = p_w \exp(\mp ik_w z)$, $\tau(z,z') = (z-z')/v_\parallel$, $\omega_b^2 \equiv 4\pi e^2 n_b/m$,

$$D_{\pm} \equiv -\exp(\pm i\Omega_0\tau(z)) \left(\delta\hat{A}_{\pm}(z) - \delta\hat{A}_{\pm}(0)\exp(i(\omega\mp\Omega_0)z/v_z) \right.$$

$$\left. \mp i\frac{\Omega_0}{v_z}\int_0^z dz'\delta\hat{A}_{\pm}(z')\exp(i(\omega\mp\Omega_0)\tau(z,z')) \right), \qquad (29)$$

and

$$D_z \equiv \frac{\gamma mc}{p}\int_0^z dz' \exp(i\omega\tau(z,z')) \left[-\partial_z\delta\phi(z') + \frac{i\omega}{c}\left(\frac{p_-}{p_z}\delta\hat{A}_+(z') + \frac{p_+}{p_z}\delta\hat{A}_-(z')\right)\right] \qquad (30)$$

for $P_x = P_y = 0$. The dispersion equations are obtained by using these perturbed currents in the wave equations

$$\left(\partial_z^2 + \frac{\omega^2}{c^2}\right) \delta\hat{A}_{\pm}(z) = -\frac{4\pi}{c}\ \delta\hat{J}_{\pm},$$

$$\partial_z\ \delta\hat{\phi}(z) = \frac{8\pi i}{\omega}\ \delta\hat{J}_z. \tag{31}$$

We are primarily interested in the low gain, tenuous beam limit in which $\omega_b << \omega$ and the wave amplitudes vary little over the length of the interaction region. This is the regime appropriate to the experiments conducted at Stanford University.[1,2] In this regime collective effects are unimportant and the space-charge potential can be neglected. In addition, the coupling between the electromagnetic modes described by $\delta\hat{A}_+$ and $\delta\hat{A}_-$ scales with p_w^2/p_z^2. However, the assumption of low gain implies that this parameter is small, and we can focus attention on one or the other of these modes exclusively. We choose to consider $\delta\hat{A}_+$, which in the low gain regime can be represented as

$$\delta\hat{A}_+(z) = \delta\hat{A}_+(0)\exp\left(i\int_0^z dz' k_+(z')\right)\ , \tag{32}$$

where $|\mathrm{Im}k_+(z)| << |\mathrm{Re}k_+(z)|$. Under the assumption that $k_+(z) = k + \delta k_+(z)$, where k is independent of axial position and $|\delta k_+(z)/k| << 1$, the dispersion equation becomes

$$k^2 - \omega^2/c^2 \simeq 0, \tag{33}$$

and

$$\begin{aligned}
\mathrm{Im}\delta k_+(z) \simeq -\frac{\omega_b^2}{2kc^2}\int_0^\infty dp \Bigg\{ & \frac{1}{2} m\omega\beta_w^2 \frac{\sin(\omega/v_{||} - k - k_w)z}{\omega/v_{||} - k - k_w} \frac{\partial}{\partial p} \\
& + \frac{p}{\gamma p_z} \frac{\beta_w^2}{2}\left[\frac{\omega}{k_w v_{||} - \Omega_0} - \frac{\Omega_0}{\omega - (k+k_w)v_{||}}\left(1 - \frac{\omega-\Omega_0}{k_w v_{||} - \Omega_0}\right)\right. \\
& \left. + \frac{\Omega_0^2}{(k_w v_{||} - \Omega_0)(\omega - \Omega_0 - kv_{||})}\right] \sin(\omega/v_{||} - k - k_w)z \\
& - \frac{p}{\gamma p_z}\left[1 + \frac{\beta_w^2}{2}\left(1 + \frac{\omega}{k_w v - \Omega_0}\right)\right]\frac{\omega - kv_{||}}{\omega - \Omega_0 - kv_{||}} \sin(\omega/v_{||} - \Omega_0/v_{||} - k)z \Bigg\} G_b(p),
\end{aligned} \tag{34}$$

where $\beta_w^2 \equiv p_w^2/p_z^2$. This result reduces to that found by Sprangle and Smith[4] in the limit of a vanishing axial magnetic field.

The total gain over an interaction region of length L is defined as $G_L \equiv -\int_0^L dz' \mathrm{Im}\delta k_+(z)$. Integrating (34), therefore, we find

$$\begin{aligned}
G_L \simeq -\frac{\omega_b^2 L}{2kc^2}\int_0^\infty dp G_b(p) \Bigg\{ & \frac{m\omega L}{4}\frac{\partial}{\partial p}\left(\beta_w^2 \frac{\sin^2\theta_w}{\theta_w^2}\right) \\
& - \frac{p}{\gamma p_z}\frac{\beta_w^2}{2}\frac{\omega}{k_w v_{||} - \Omega_0}\left(1 + \frac{\Omega_0 L}{2v_{||}}\frac{\Omega_0}{\omega\theta_g}\right)\frac{\sin^2\theta_w}{\theta_w} + \frac{p}{\gamma p_z}\frac{\beta_w^2}{2}\frac{\Omega_0 L}{2v_{||}}\left(1 - \frac{\omega + \Omega_0}{k_w v_{||} - \Omega_0}\right)\frac{\sin^2\theta_w}{\theta_w^2} \\
& - \frac{p}{\gamma p_z}\left[1 + \frac{\beta_w^2}{2}\left(1 + \frac{\omega}{k_w v_{||} - \Omega_0}\right)\right]\left(\theta_g + \frac{\Omega_0 L}{2v_{||}}\right)\frac{\sin^2\theta_g}{\theta_g^2} \Bigg\},
\end{aligned} \tag{35}$$

where $\theta_w \equiv (\omega/v_{||}-k-k_w)L/2$ and $\theta_g \equiv (\omega/v_{||}-\Omega_0/v_{||}-k)L/2$. If the beam is sufficiently cold that a distribution of the form

$$G_b(p) = \frac{p_z}{p}\ \delta(p-p_0) \tag{36}$$

can be used, then the total gain becomes

$$G_L \simeq \frac{\omega_b^2}{2kc^2}\ \frac{L}{\gamma_0}\ \Bigg\{ \frac{\beta_{w0}^2}{2}\ \Bigg[\frac{\omega^2 L^2}{4\gamma_{z0}^2 v_{||0}^2} \left(1 - \frac{\gamma_{z0}^2\beta_{w0}^2\Omega_0}{\Omega_0(1+\beta_{w0}^2)-k_w v_{||0}}\right) \frac{\partial}{\partial\theta_{w0}} \left(\frac{\sin\theta_{w0}}{\theta_{w0}}\right)^2$$

$$- k_w L \left(\frac{\omega}{\Omega_0(1+\beta_{w0}^2)-k_w v_{||0}} + \frac{\Omega_0}{2k_w v_{||0}} \left(1 - \frac{\omega+\Omega_0}{k_w v_{||0}-\Omega_0}\right)\right) \left(\frac{\sin\Omega_{w0}}{\theta_{w0}}\right)^2 \tag{37}$$

$$+ \frac{\omega}{k_w v_{||0}-\Omega_0} \left(1 + \frac{\Omega_0}{\omega}\ \frac{\Omega_0 L}{2v_{||0}}\ \frac{1}{\theta_{g0}}\right) \frac{\sin^2\theta_{w0}}{\theta_{w0}} \Bigg]$$

$$- \left[1 + \frac{\beta_{w0}^2}{2}\left(1 + \frac{\omega}{k_w v_{||0}-\Omega_0}\right)\right] \left(1 + \frac{\Omega_0 L}{2v_{||0}}\ \frac{1}{\theta_{g0}}\right) \frac{\sin^2\theta_{g0}}{\theta_{g0}} \Bigg\}\ .$$

In Eq. (37), $\gamma_0 \equiv (1 + p_0^2/m^2c^2)^{1/2}$, $\gamma_{z0} \equiv (1 - v_{z0}^2/c^2)^{-1/2}$, $\beta_{w0}^2 \equiv p_{w0}^2/p_{||0}^2$, $p_{w0}^2 \equiv \Omega_w^2 p_{||0}^2/(\Omega_0-k_w v_{||0})^2$, and $p_{||0}$ and $v_{||0}(\equiv p_{||0}/\gamma_0 m)$ are determined by the appropriate solution to $p_0^2 = p_{w0}^2 + p_{||0}^2$. It is clear from (37), therefore, that wave amplification can occur, in principle, for frequencies corresponding to both the usual free electron laser resonance ($\omega \simeq (k+k_w)v_{||0}$) and the Doppler-shifted gyroresonance ($\omega \simeq \Omega_0 + kv_{||0}$).

If the pump period is short compared to the length of the system, the gain for frequencies $\omega \simeq (k+k_w)v_{\|0}$ is dominated by the first term in (37)

$$G_L \simeq \beta_{w0}^2 \frac{\omega_b^2 L^3 k}{16\gamma_0 \gamma_{z0}^2 v_{\|0}^2} \left(1 - \frac{\gamma_{z0}^2 \beta_{w0}^2 \Omega_0}{\Omega_0(1+\beta_{w0}^2) - k_w v_{\|0}}\right) \frac{\partial}{\partial \theta_{w0}} \left(\frac{\sin\theta_{w0}}{\theta_{w0}}\right)^2. \tag{38}$$

The extrema occur for $\theta_{w0} \simeq \pm 1.3$ at which $\partial(\sin\theta_{w0}/\theta_{w0})^2/\partial\theta_{w0} \simeq \mp .54$, which correspond to frequencies

$$\omega \simeq 2\gamma_{z0}^2 k_w v_{\|0}(1 \pm 2.6/k_w L), \tag{39}$$

and peak gains

$$(G_L)_{max} \simeq \mp .068\, \beta_{w0}^2 \frac{\omega_b^2}{\gamma_0 k_w^2 c^2} (k_w L)^3 \left(1 - \frac{\gamma_{z0}^2 \beta_{w0}^2 \Omega_0}{\Omega_0(1+\beta_{w0}^2) - k_w v_{\|0}}\right), \tag{40}$$

where the plus or minus sign must be chosen to give a positive gain in (40). These expressions for the gain are similar to those found previously[4,19-22] in the limit of zero axial field. The principal diferences between this result and those found previously are that (1) gain can occur for both frequencies shown in (39), and (2) a singularity is introduced for $k_w v_{\|0} \simeq \Omega_0(1 + \beta_{w0}^2)$ which implies that the effect of the axial guide field can be to

substantially enhance the small signal gain over the case in which no guide field is present. Note, however, that the singularity is a product of our choice of a monoenergetic beam. The inclusion of an energy spread can be expected to broaden the resonance and remove the singularity.

We now focus on the effect of the axial magnetic field on the gain for the free electron laser resonance. If Δ denotes the ratio of the gain in the presence of an axial guide field to the appropriate expression in the limit $B_0 \to 0$, then it follows that

$$\Delta = -\mu^2 \frac{\varepsilon^2\beta_v^2 + (\mu-1)[\varepsilon^2 + (\mu-1)^2\gamma_0^{-2}]}{[\varepsilon^2 - (\mu-1)^3][\varepsilon^2 + (\mu-1)^2\gamma_0^{-2}]}, \tag{41}$$

where $\mu \equiv k_w v_{\|0}/\Omega_0$, and $v_{\|0}$ must be computed in a self-consistent manner to recover the constant-v_3 solutions in (5). As a result, Δ can be expressed as a function of ε, β_v, and β_0 (where the choice of constant-v_3 solutions implicitly selects β_u). With these considerations in mind we plot Δ versus β_0 for fixed values of total electron energy and wiggler period and amplitude in Fig. 9c. We shall restrict consideration to stable uniform-v_3 trajectories propagating parallel to the axial guide field. We choose $\beta_v = .97$ and $\Omega_w/k_w c = .07$ and plot the variation in $v_{\|0}$ with β_0 in Fig. 9a. Evidently there is a stable high axial velocity trajectory (orbit I) in the low-β_0 regime ($\lesssim .72$ for the chosen parameters), as well as a trajectory which varies widely in magnitude with β_0 (orbit II). Since the frequency of the amplified modes scale approximately as $v_{\|0}$, an electron beam characterized by trajectories in group I can be expected to excite high frequency waves for all accessible values of β_0. In contrast, trajectories

in group II can give rise to a wide spectrum of oscillations and, for the chosen parameters, and high frequency waves will result only for $\beta_0 \gtrsim 1$. This is clearly shown in Fig. 9b in which we plot the resonant frequency versus β_0 for both classes of orbits. The significant feature which we are concerned with, however, is the effect of the axial guide field on the small-signal gain. To this end, we plot Δ versus β_0 in Fig. 9c for the stated parameters. We observe, first, that $\Delta \geq 1$ throughout the entire range of β_0 accessible to orbits in group I and, hence, the gain is enhanced relative to the zero axial field ($\beta_0 \to 0$) limit. In addition, significant enhancements in the gun are possible near the indicated resonance at

$$\beta_0 = (1 + \varepsilon^{2/3})^{-1} \frac{v_{\|0}}{c} , \tag{42}$$

which is the orbital stability boundary discussed previously in the regime in which $\beta_0 < v_{\|0}/c$. The resonance condition is not found for orbits in group II, however, since $\beta_0 > v_{\|0}/c$ for all such trajectories. Indeed, Δ vanishes for $\beta_0 \approx 1.39$ in the range of axial fields studied. Enhancement in the gain for these orbits occurs only for limited ranges of β_0. A significant enhancement is found in the low-β_0 regime (i.e., $.1 \lesssim \beta_0 \lesssim 1.34$), but corresponds to comparatively low frequency waves (see Fig. 9b). Enhancements in the gain for high frequency waves is found only for a limited range of axial field strengths ($1.45 \lesssim \beta_0 \lesssim 1.8$), but is at most of the order of 35%.

The enhancement in the gain for axial fields such that β_0 is of the order of unity is readily explained from consideration of the behavior of

v_w. It is clear that for axial fields in which $\Omega_0 \sim k_w v_{\|0}$ (i.e., $\beta_0 \sim 1$) large enhancements in the wiggle velocity v_w occur. This is the source in the enhancements in both the gain and emissivity. However, as $\underset{\sim}{B}_0$ continues to increase $v_w \to \varepsilon v_{\|0}$ and the wiggle velocity decreases relative to that found in the zero axial field limit.

In the absence of an axial guide field the small signal gain scales as the square of the wiggler amplitude (i.e., $\Omega_w^2/k_w^2c^2$) which is also the square of the wiggle velocity. However, for finite values of the axial guide field this variation is more complex and the gain does not increase monotonically with either Ω_w/k_wc or the wiggle velocity. This situation is illustrated in Fig. 10, in which we plot the peak gain (solid line) and frequency corresponding to peak gain (dashed line) versus Ω_w/k_wc for $\beta_0 = 1.13$ and $v/c = .96$. For small values of this parameter the gain does indeed scale as the square of the wiggler amplitude, but a peak occurs at $\Omega_w/k_wc \simeq .012$ after which the gain rapidly drops to zero. In addition the frequency monotonically decreases throughout. Note that while Ω_w/k_wc does not equal the wiggle velocity in the presence of an axial field, the decreasing frequency implies a decreasing axial velocity which, in turn, leads to an increasing wiggle velocity. This is illustrated more clearly in Fig. 11 in which we plot the variation in the axial velocity versus Ω_w/k_wc for $v/c = .96$ and $\beta_0 = .75$ and 1.13. For $\beta_0 = 1.13$ all orbits are of group II class and the axial velocity is a decreasing function of Ω_w/k_wc over the range studied. Since this means that the wiggle velocity increases with the wiggler amplitude over this range, it must be concluded that the small signal gain cannot necessarily be increased by a simple enhancement in the wiggle velocity.

For sufficiently smaller values of β_0, group I orbits appear (see Fig. 11 for $\beta_0 = .75$) over a limited range of wiggler field amplitudes. The peak gain (as well as the corresponding frequency) for this case is shown in Fig. 12, and describes the frequency and gain associated with the group I orbits. We have restricted consideration to group I orbits, because while group II orbits also lead to growth, the gain is weaker and the frequency is relatively low ($\omega \lesssim 8\, k_w c$). For these orbits, the gain is seen to increase with increasing wiggle velocity, and the singularity mentioned previously is also found at the transition to orbital instability. It should be remarked, however, that the small signal approximation breaks down in the vicinity of the singularity.

The gain for gyroresonant emission is given by ($\omega \simeq \Omega_0 + kv_{\|0}$)

$$G_L \simeq -\frac{\omega_b^2}{2kc^2}\,\frac{L^2\Omega_0}{\gamma_0 v_{\|0}}\left[1 + \frac{\beta_{w0}^2}{2}\left(1 + \frac{\omega}{k_w v_{\|0} - \Omega_0}\right)\right]\frac{\sin^2\theta_{g0}}{\theta_{g0}^2}\,, \tag{43}$$

for a long interaction region ($k_w L \gg 1$), and growth is possible if $k_w v_{\|0} \lesssim \Omega_0$ and

$$\beta_{w0}^2 \gtrsim \frac{(\Omega_0 - k_w v_{\|0})}{(k + k_w) v_{\|0}} \tag{44}$$

Peak amplification occurs at the maximum of $(\sin\theta_{g0}/\theta_{g0})^2 \simeq 1$, which corresponds to a frequency $\omega = \Omega_0 + kv_{\|0}$ and peak gain

$$(G_L)_{max} \simeq \frac{\omega_b^2 L^2}{2\gamma_0 c^2}\left(\frac{\beta_{w0}^2}{2}\,\frac{(1 - v_{\|0}/c)\gamma_{z0}^2\Omega_0 + k_w c}{\Omega_0 - k_w v_{\|0}} - \frac{c}{v_{\|0}}\right) \tag{45}$$

The variation of the peak gain and associated frequency for gyroresonant emission with axial field strength are shown in Fig. 13 for parameters consistent with the calculation of the frequency and peak gain at the free electron laser resonance presented in Fig. 9. Gyroresonant emission is found only for group II orbits and, as expected, the frequency increases with increasing β_0. In contrast, the gain is found to decrease with increasing axial field strengths. The large increase in the gain as β_0 approaches zero results from the fact that $v_{\|0}$ also vanishes in this limit. However, the small signal gain approximation breaks down in this limit, and nonlinear effects can be expected to produce enhancements lower than expected on the basis of the linearized theory.

V. SUMMARY AND DISCUSSION

In this work, we have considered both the spontaneous and induced emission from a free electron laser in which a uniform axial guide field is present. The existence of the axial field is found to introduce an additional source of coupling between the axial and transverse electron motion which, for sufficiently strong field levels (14), can lead to orbital instability for motion parallel to $\underset{\sim}{B}_0$. Since the existence of orbital instability results in a rapid dispersal of an initially bunched electron beam with disastrous implications for the expected radiation levels, we focus attention on the parameter regimes corresponding to orbital stability and orbits characterized by nearly uniform axial velocities. The predominant transverse motion of these orbits is to track the wiggler field; however, a relatively small component of Larmor rotation associated with the guide field may also be present. Because of this, emission can be expected for both the free electron laser and gyrotron resonance conditions.

The spontaneous emission describes the ambient level of noise within the device prior to the coherent amplification process. As shown in Eq. (21), the spontaneous emissivity for waves propagating axially contains components due to the transverse motion resulting from the action of the wriggler and axial guide fields. In each case the level of emission is proportional to the square of the magnitude of the transverse velocities. This velocity corresponds to the canonical momentum in the transverse direction for the gyrotron mode ($\omega \simeq \Omega_0 + kv_{||}$), and to the wiggler velocity v_w for the free electron laser mode

($\omega \simeq (k+k_w)v_{\parallel}$). It should be recognized that the presence of a finite β_0 leads to an enhancement in v_w and, consequently, in the free electron laser emissivity by a factor of $(\Omega_0/k_w v_{\parallel} - 1)^{-2}$. As discussed in Sec. IV the limit in which $\Omega_0 = k_w v_{\parallel}$ is not achievable.

Enhancement in the linearized (or small signal) gain also expected to result when an axial guide field is present. For the tenuous beam, low gain regime the enhancement of the gain is expected to be greatest for parameters in the vicinity of the transition to orbital instability (denoted by the dashed line in Fig. 9) which corresponds to a beam characterized by orbital stability. In order for the analysis to be valid for orbitally stable beams, however, stringent requirements on beam quality must be satisfied because a small energy spread can lead to a rapid breakdown in the coherence of the beam. In addition, the small-signal gain approximation must break down in the vicinity of the resonance (i.e., the transition to orbital instability). Finally, significant enhancements in the gain are expected to occur for low wavelength oscillations only in the low-β_0 regime.

ACKNOWLEDGMENTS

This work was supported, in part, under NAVAIR contract WF32-389-592. One of us (H.P.F.) would like to thank the Instituto de Fisica of the Universidade Federal do Rio Grande do Sul for hospitality during his visit in the fall of 1980. In addition, support for several of us (D.D., E.H.J., B.L., and R.S.S.) was provided by Conselho Nacional de Desenvolvimento Cientifico e Tecnologico and Financiadora de Estudos e Projetos.

REFERENCES

1. L. R. Elias, W. M. Fairbank, J. M. J. Madey, H. A. Schwettman, and T. I. Smith, Phys. Rev. Lett. 36, 717 (1976).

2. D. A. G. Deacon, L. R. Elias, J. M. J. Madey, G. J. Ramian, H. A. Schwettman, and T. I. Smith, Phys. Rev. Lett. 38. 892 (1977).

3. D. B. McDermott, T. C. Marshall, S. P. Schlesinger, R. K. Parker, and V. L. Granatstein, Phys. Rev. Lett. 41, 1368 (1978).

4. P. Sprangle and R. A. Smith, Phys. Rev. A 21, 293 (1980).

5. I. B. Bernstein and J. L. Hirschfield, Phys. Rev. A 20, 1661 (1979).

6. R. C. Davidson and H. S. Uhm, Phys. Fluids 23, 2076 (1980).

7. T. Kwan and J. M. Dawson, Phys. Fluids 22, 1089 (1979).

8. M. Zales Caponi, J. Munch, and M. Boehmer, in Free-Electron Generators of Coherent Radiation (eds. S. F. Jacobs, H. S. Pilloff, M. Sargent, M. O. Scully, and R. Spitzer, Addison-Wesley, New York, 1980), p. 523.

9. L. Friedland and J. L. Hirschfield, Phys. Rev. Lett. 44, 1456 (1980).

10. I.B. Bernstein and L. Friedland, Phys. Rev. A 23, 816 (1981).

11. L. Friedland and J.L. Hirschfield, Phys. Rev. Lett. 44, 1456 (1980).

12. J.P. Blewitt and R. Chasman, J. Appl. Phys. 48, 2692 (1977).

13. P. Diament (to be published).

REFERENCES (Continued)

14. R.C. Davidson and H.S. Uhm (to be published).

15. H.P Freund and A.T. Drobot, Phys. Fluids (submitted for publication).

16. L. Friedland, Phys. Fluids 23, 2376 (1980).

17. R.E. Shefer and G. Bekefi, Bull. APS 25, 911 (1980).

18. J.M. Buzzi, K. Fetch, and L. Vallier, Bull. APS 25, 887 (1980).

19. V.P. Sukhatme and P.W. Wolfe, J. Appl. Phys. 44, 2331 (1973).

20. W.B. Colson, Phys. Lett. 59A, 187 (1976).

21. F.A. Hopf, P. Meystre, M.O. Scully, and W.H. Louisell, Optics Comm. 18, 413 (1976).

22. N.M. Kroll and W.A. McMullin, Phys. Rev. A 17, 300 (1978).

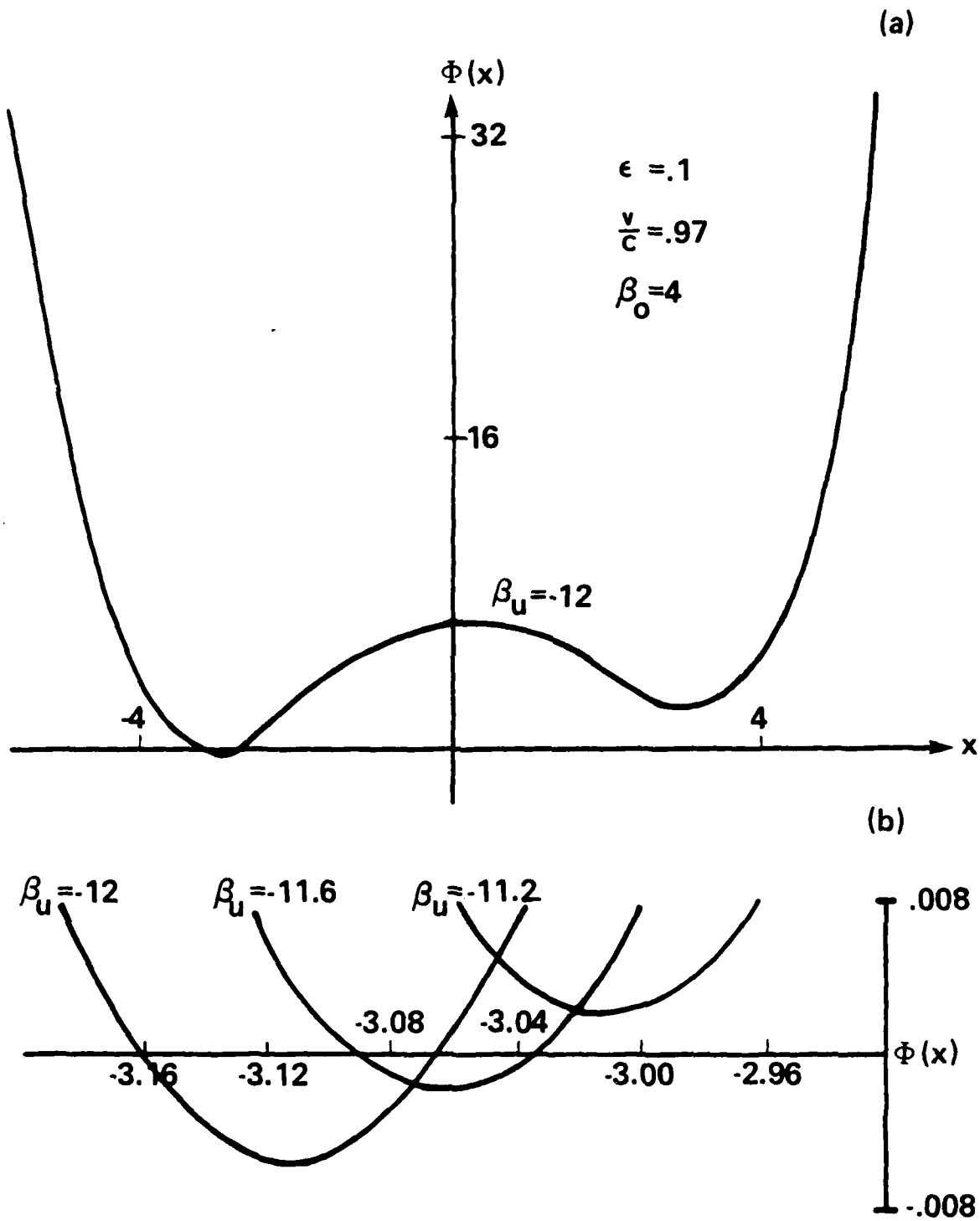

Fig. 1 — Graph of the pseudopotential Φ versus x for $\epsilon = .1$, v/c = .97 and several values of β_u.

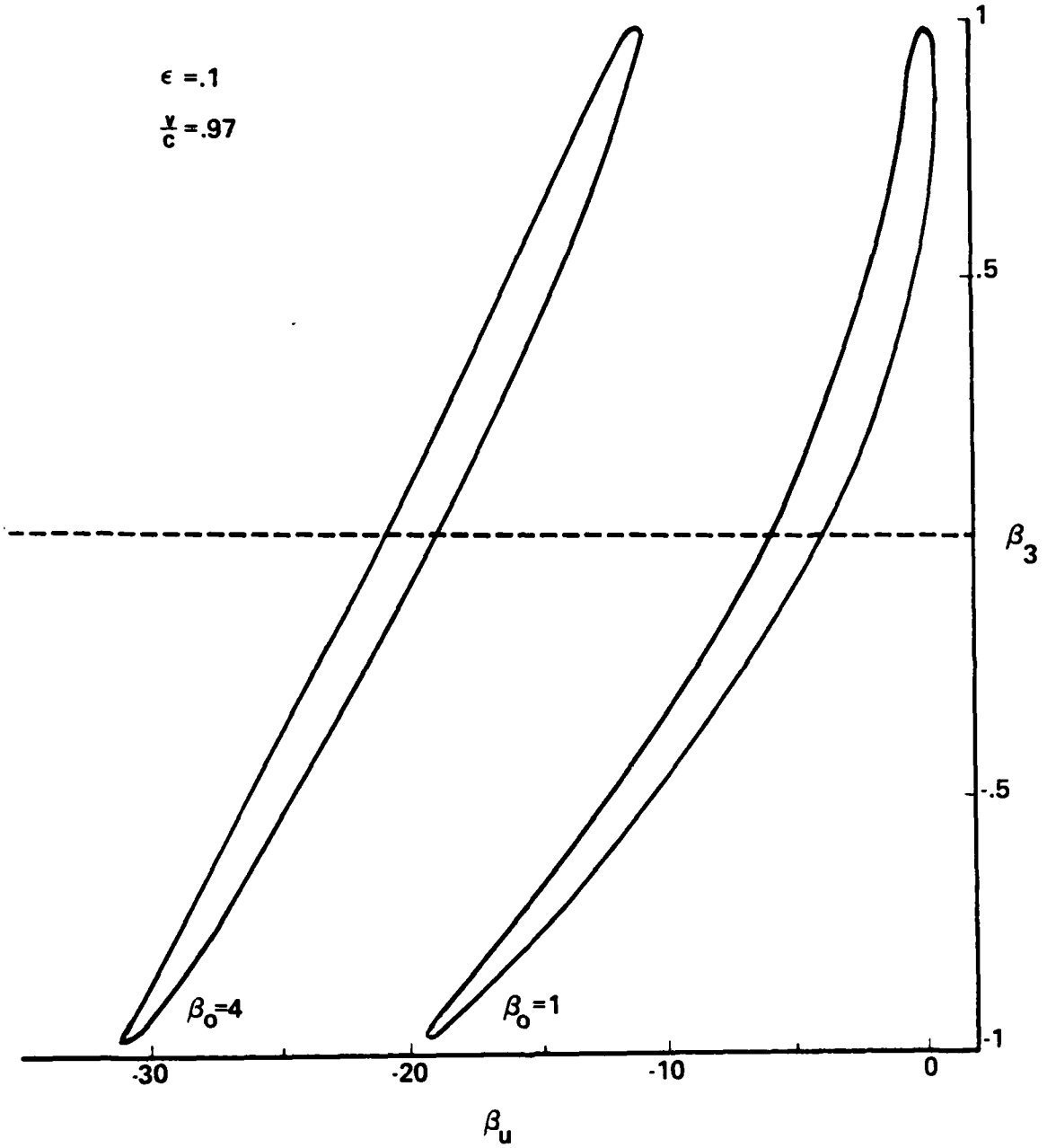

Fig. 2 - Graph of the bounds on the axial velocity versus β_u for ϵ = .1, v/c = .97, and β_0 = 1,4.

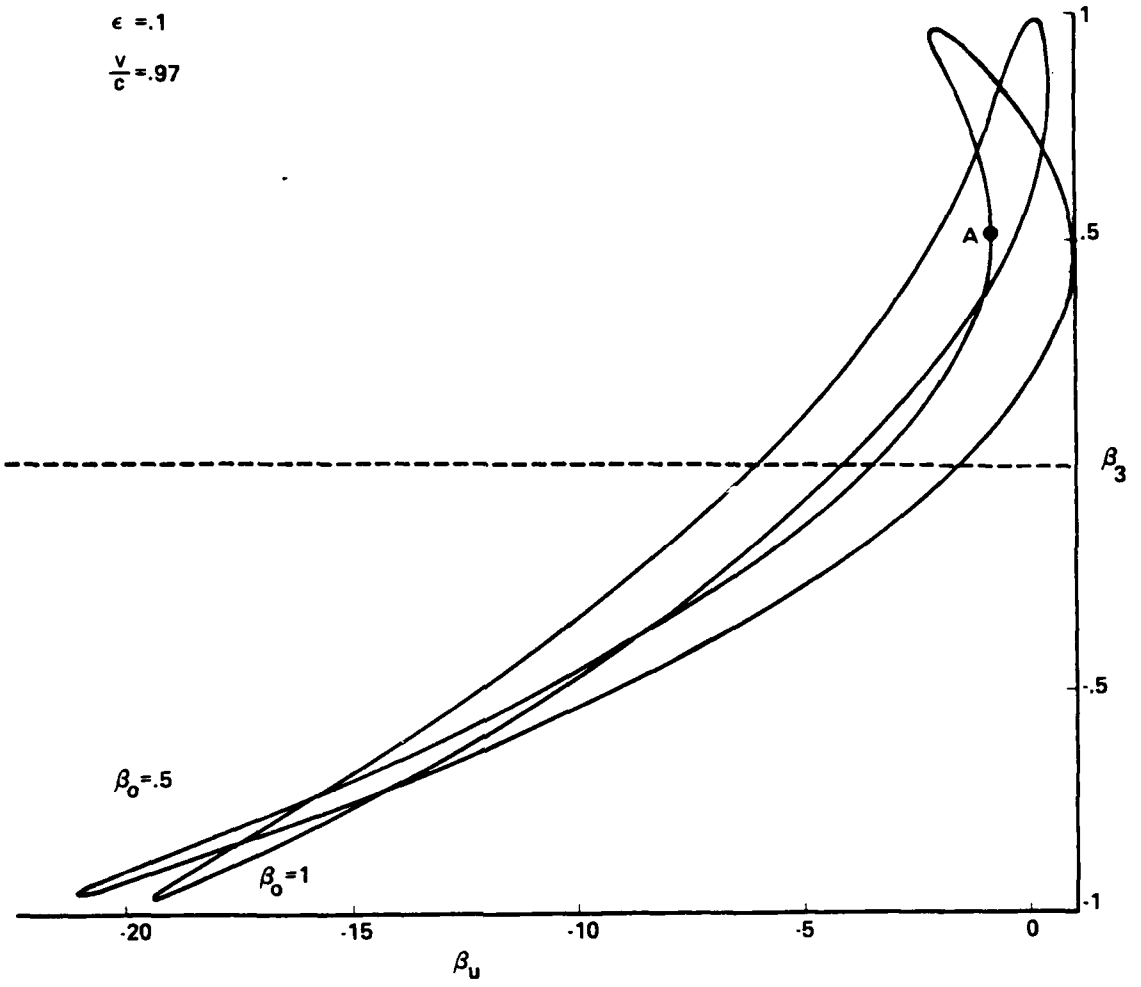

Fig. 3 - Graph of the bounds on the axial velocity versus β_u for ϵ = .1, v/c = .97, and β_0 = .5,1.

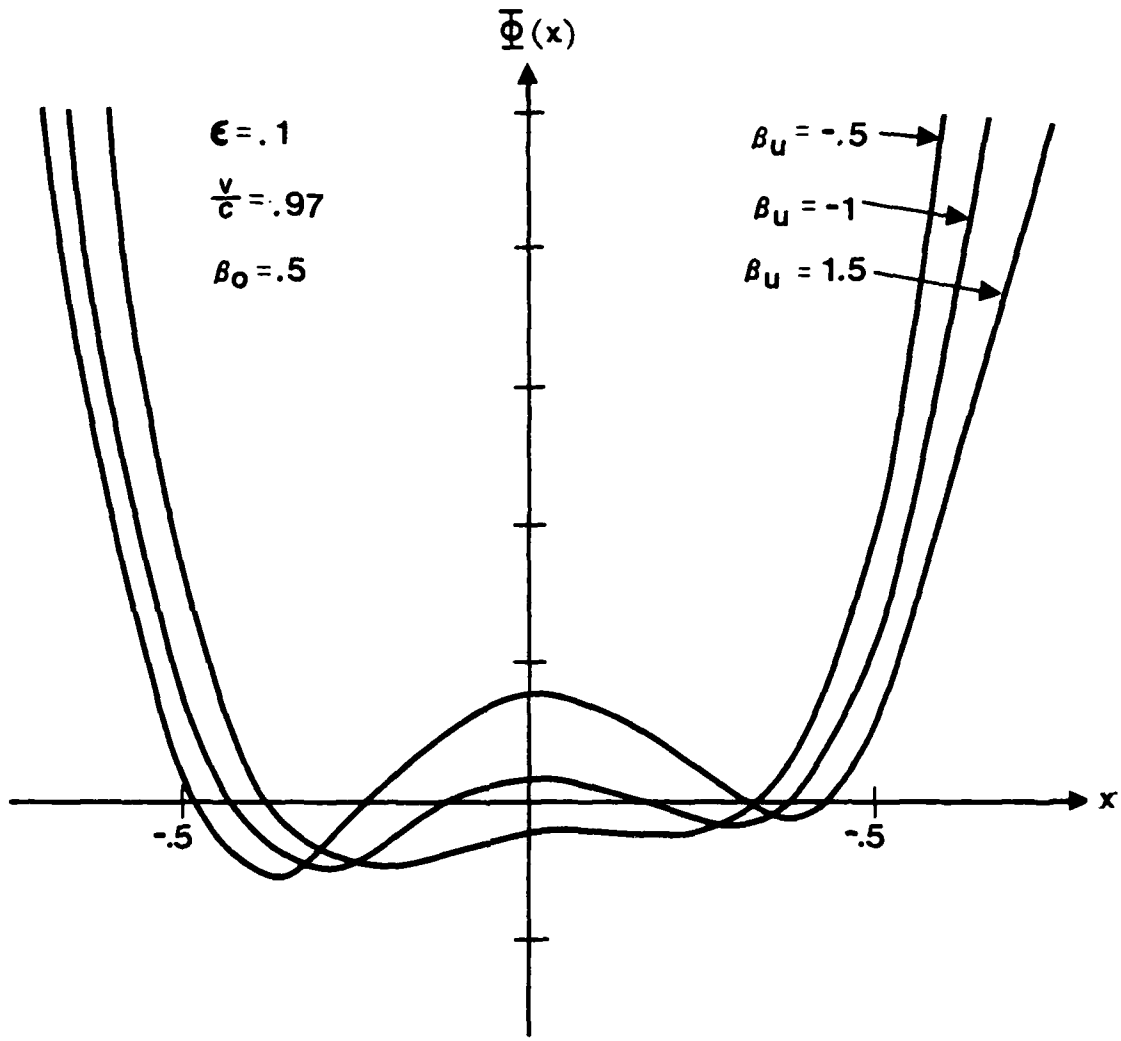

Fig. 4 - Graph showing the variation of the pseudopotential with β_u in the vicinity of an orbitally unstable uniform-v_3 trajectory.

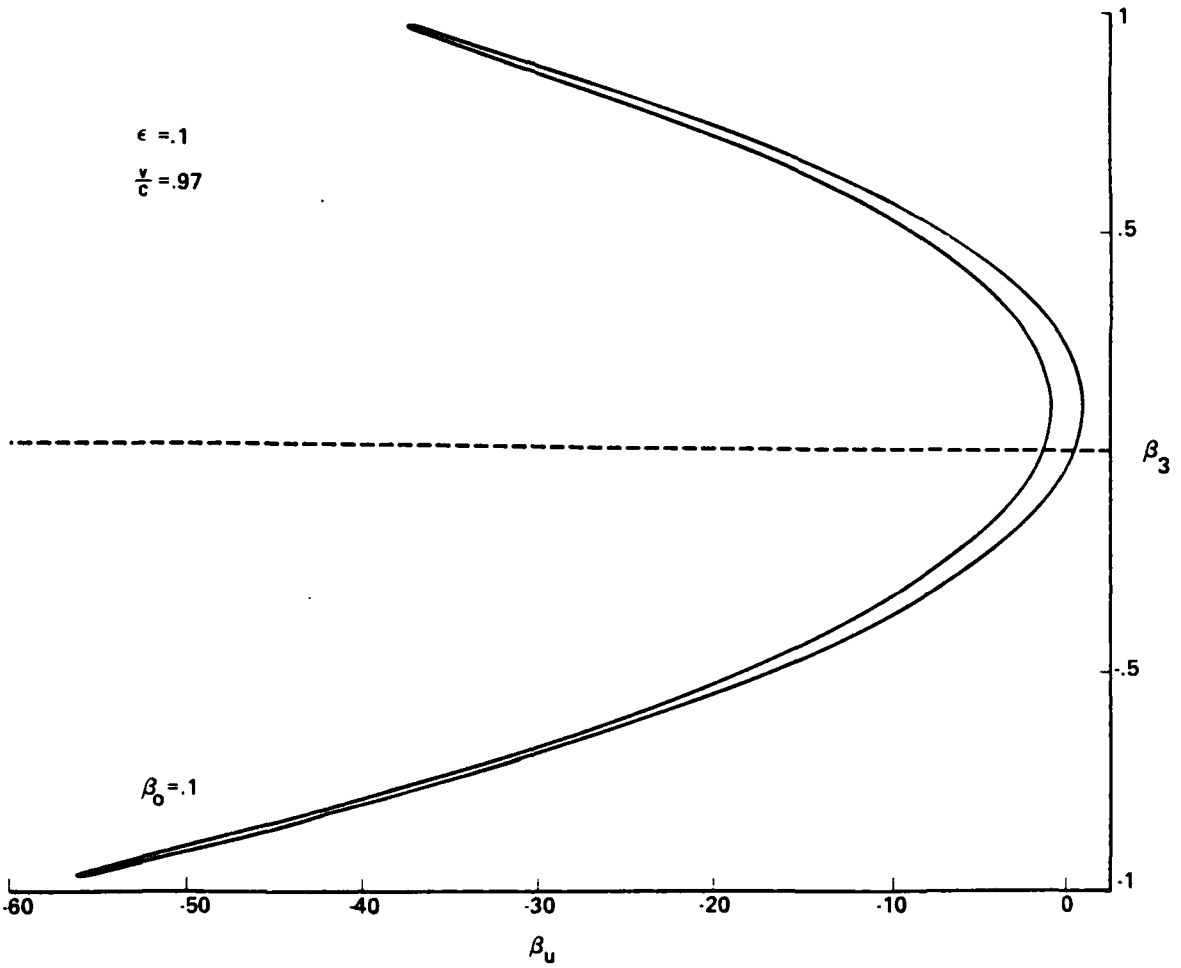

Fig. 5 - Graph of the bounds on the axial velocity versus β_u for $\varepsilon = .1$, $v/c = .97$, and $\beta_0 = .1$.

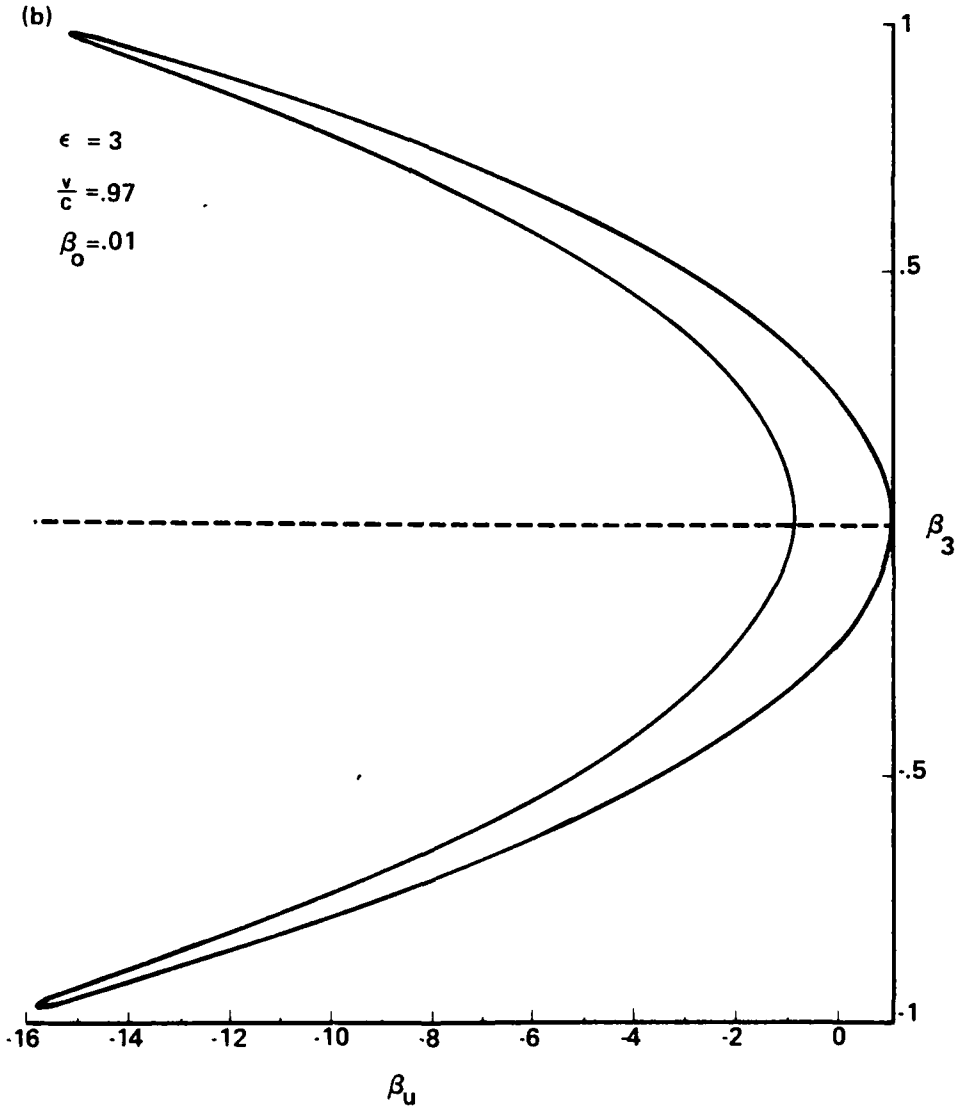

Fig. 6 - Graph of the bounds on the axial velocity versus β_u for $\varepsilon = 3$, $v/c = .97$ and $\beta_0 = .01$.

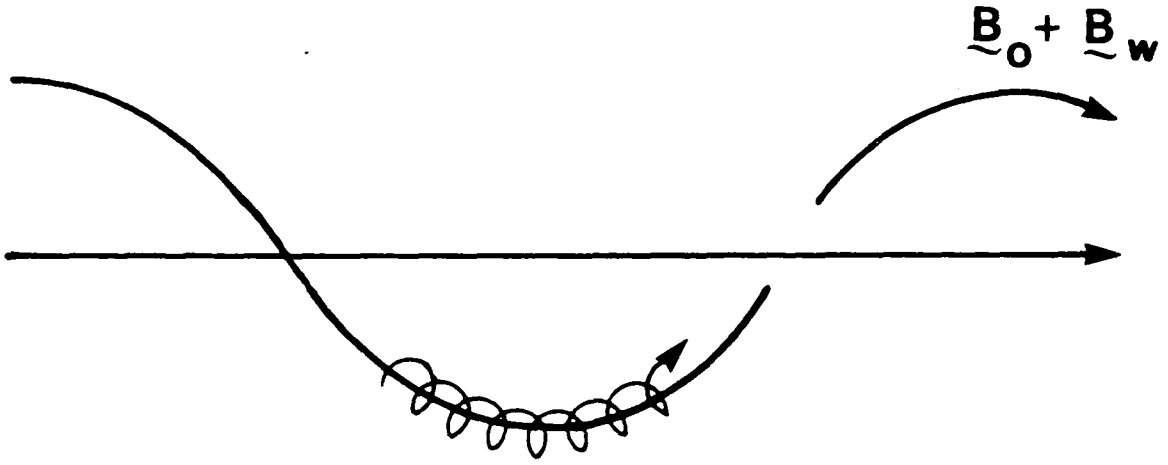

Fig. 7 - Schematic representation of the single-particle trajectories.

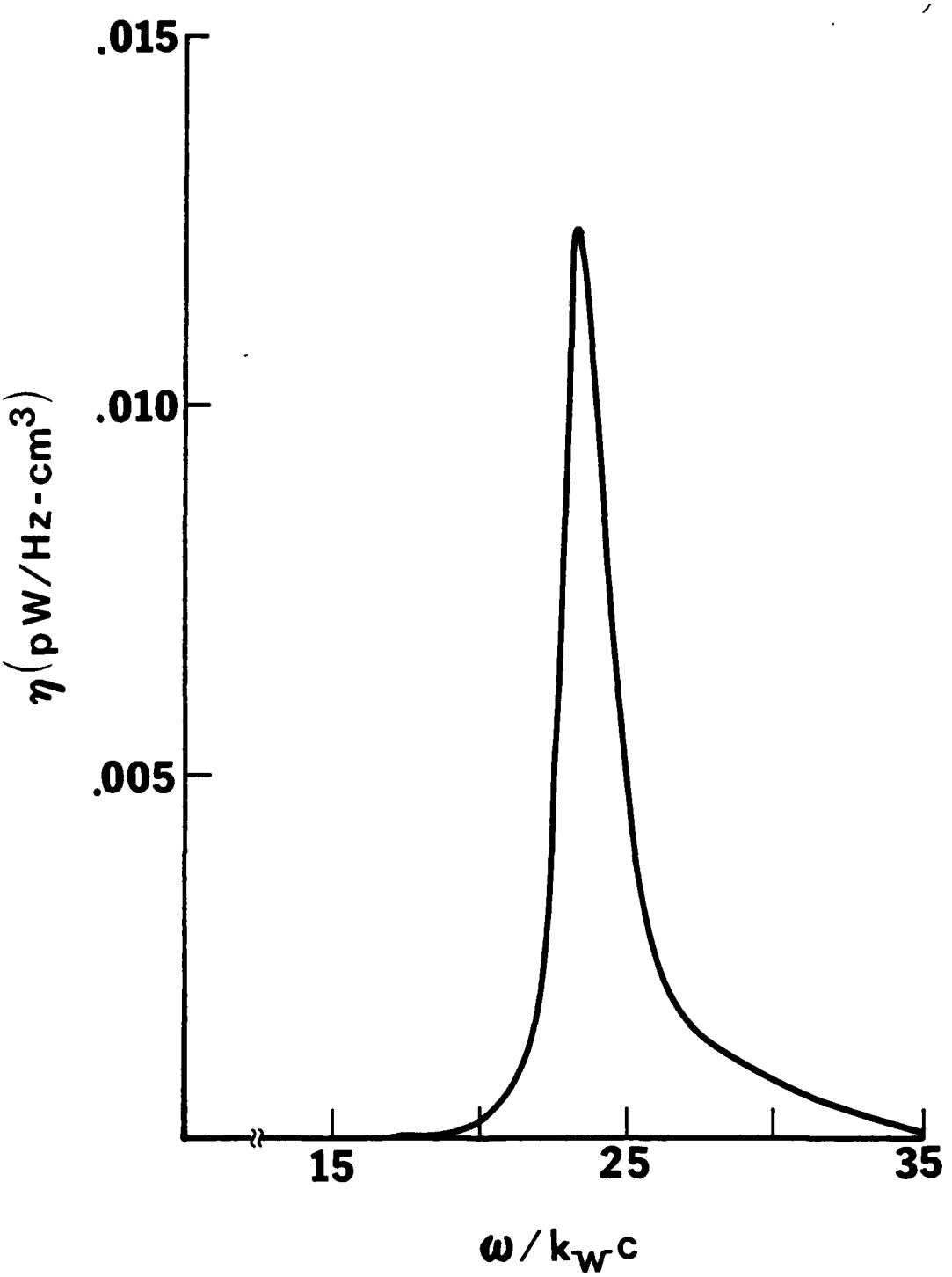

Fig. 8 - Graph of the emissivity versus frequency for propagation parallel to the axial guide field.

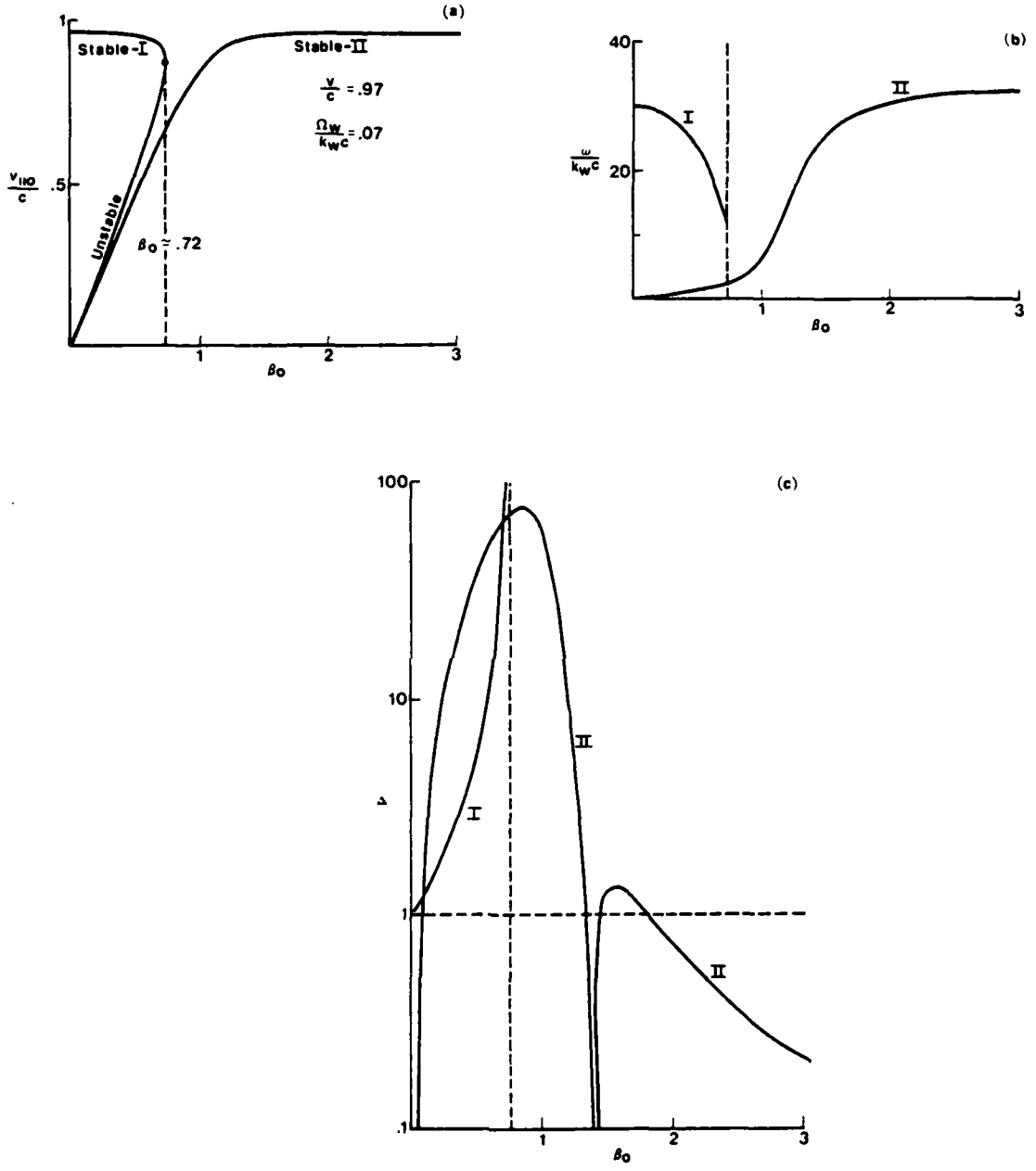

Fig. 9 - Graphs of axial velocity, and resonant frequencies and enhancements in the gain for stable trajectories versus β_0 for $v/c = .97$ and $\Omega_w/k_w c = .07$.

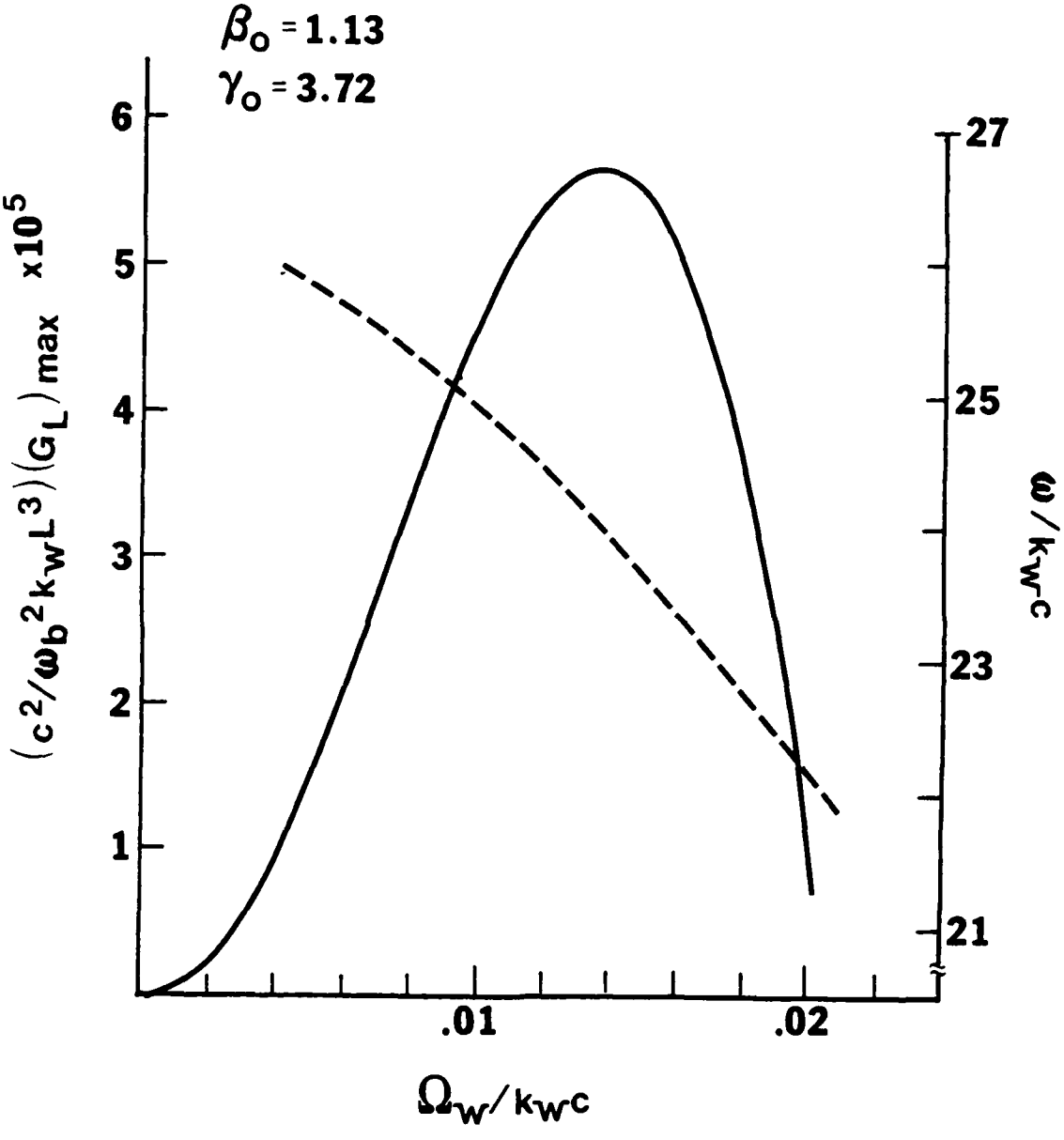

Fig. 10 - Graphs of the maximum gain (solid line) and the corresponding frequency (dashed line) versus wiggler strength for β_0 = 1.13 and v/c = .96.

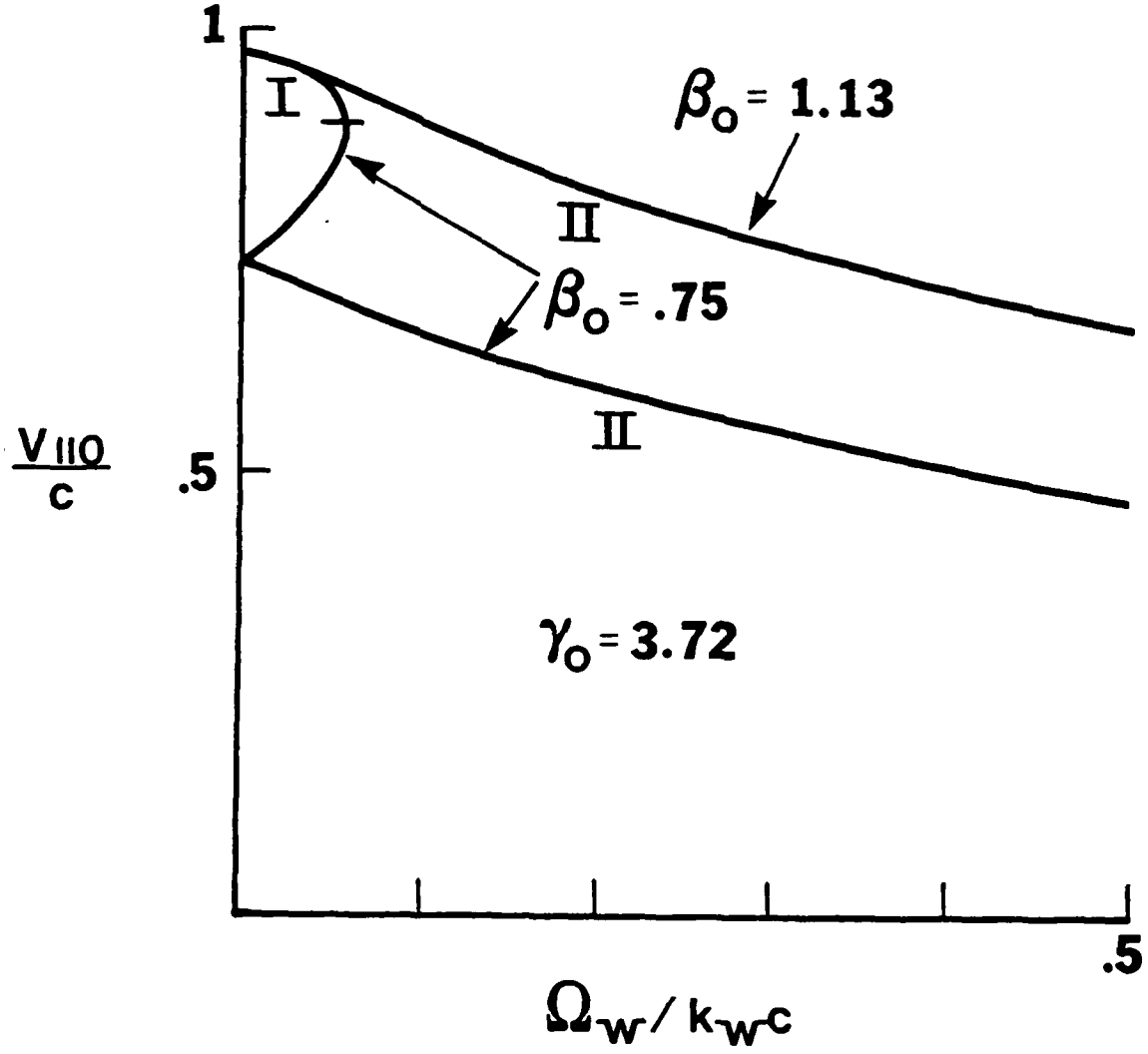

Fig. 11 - Graph of the axial velocity versus $\Omega_w/k_w c$ for v/c = .96 and β_0 = .75, and 1.13.

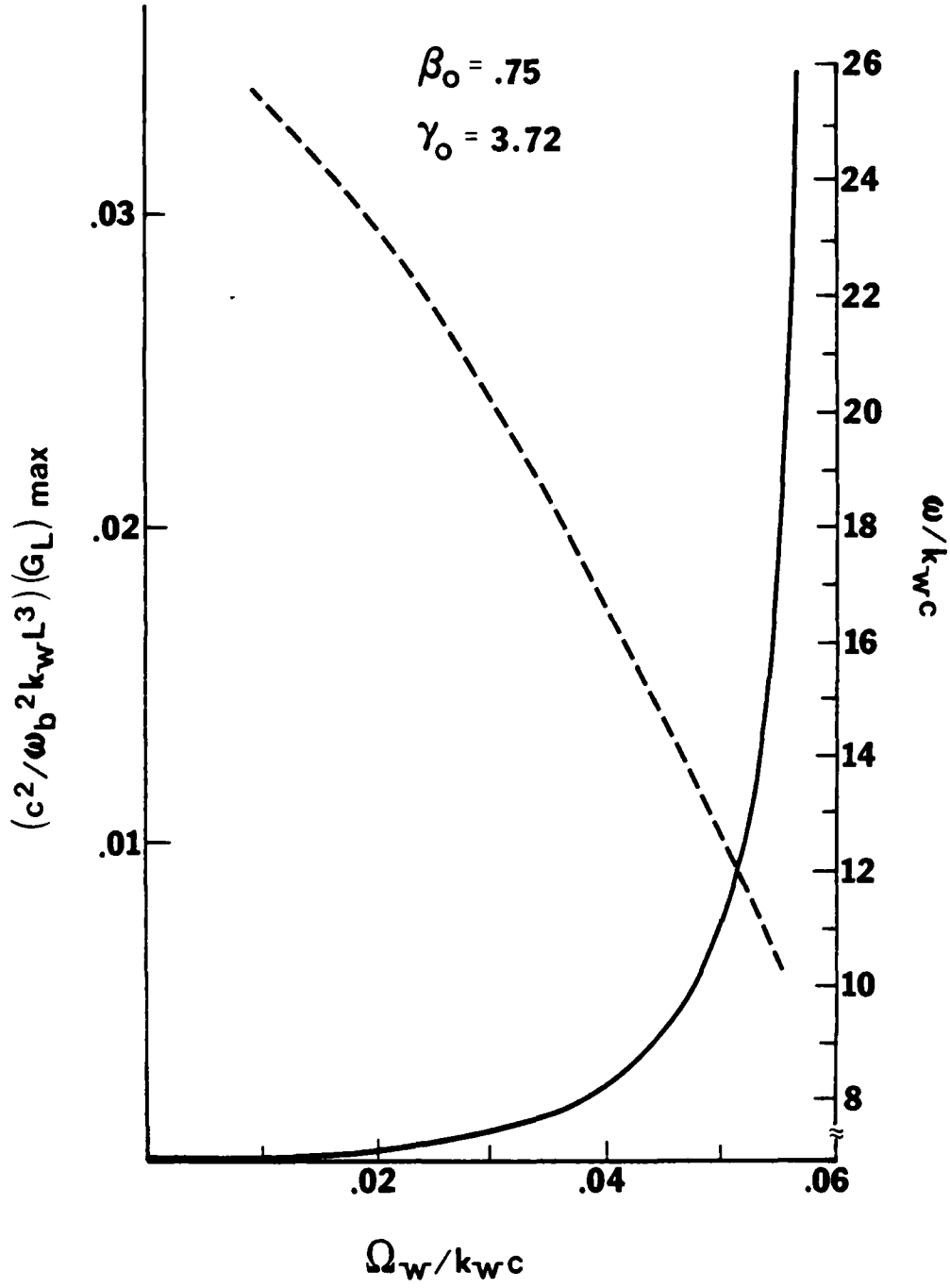

Fig. 12 - Graphs of the maximum gain and corresponding frequency for $\beta_0 = .75$ and v/c = .96.

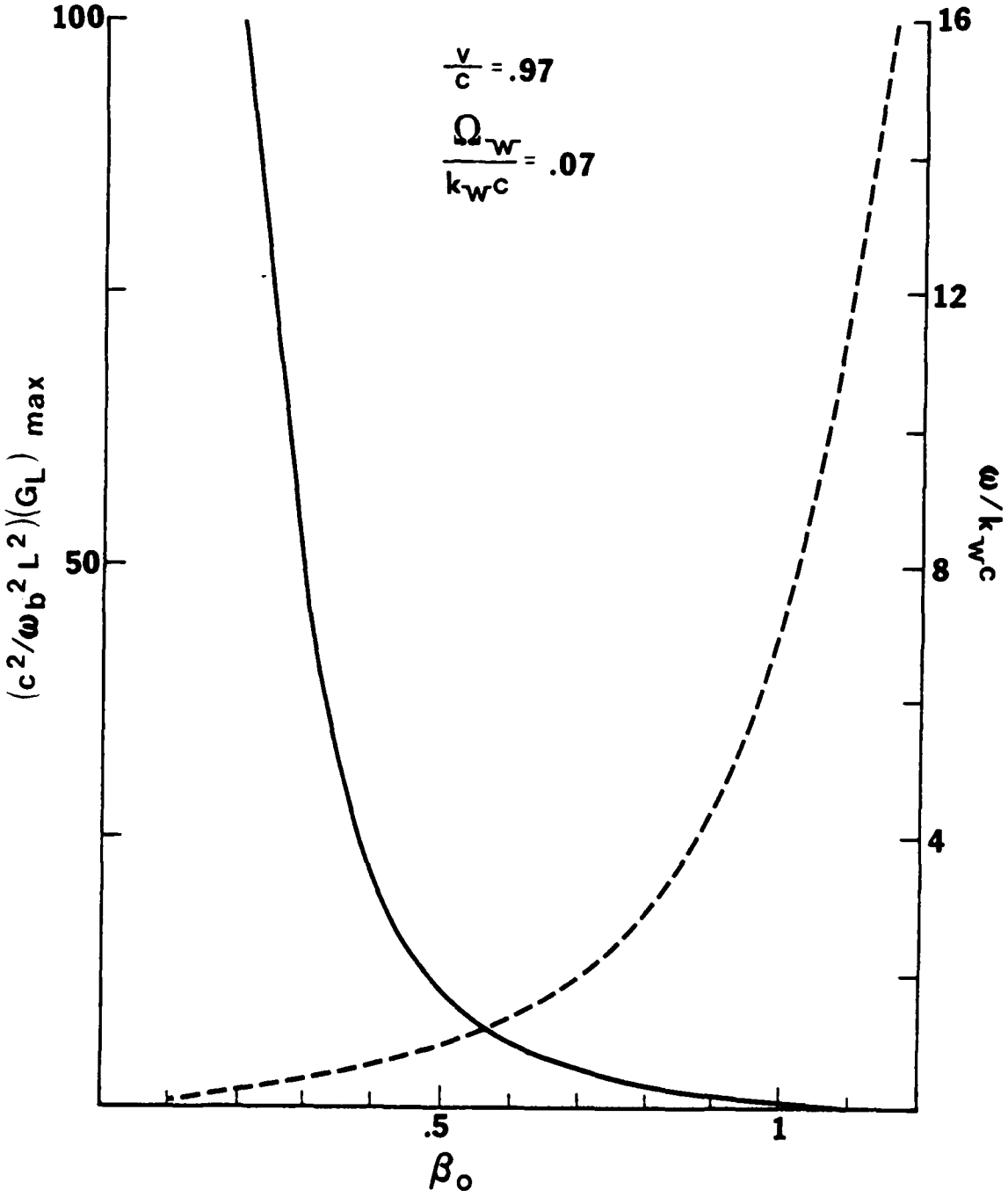

Fig. 13 - Graph of the maximum gain and associated frequency versus β_0 for cyclotron emission.

DISTRIBUTION LIST*

Naval Research Laboratory
4555 Overlook Avenue, S.W.
Washington, D.C. 20375

Attn: Code 1000 - CAPT. E. E. Henifin
1001 - Dr. A. Berman
4700 - Dr. T. Coffey (26 copies)
4701 - Mr. J. Brown
4740 - Dr. V. L. Granatstein (20 copies)
4740 - Dr. R. K. Parker (20 copies)
4740 - Dr. K. R. Chu
4740 - Dr. C. W. Roberson
4790 - Dr. P. Sprangle (100 copies)
4790 - Dr. C. M. Tang
4790 - Dr. M. Lampe
4790 - Dr. W. M. Manheimer
6603S- Dr. W. W. Zachary
6650 - Dr. L. Cohen
6656 - Dr. N. Seeman
6850 - Dr. L. R. Whicker
6805 - Dr. S. Y. Ahn
6875 - Dr. R. Wagner

On Site Contractors:
Code 4740 - Dr. L. Barnett (B-K Dynamics)
4740 - Dr. D. Dialetis (SAI)
4740 - Dr. Y. Y. Lau (SAI)
4790 - Dr. A. T. Drobot (SAI)
4790 - Dr. J. Vomvoridis (JAYCOR)
4790 - Dr. H. Freund (SAI)

* Every name listed on distribution gets one copy except for those where extra copies are noted.

Dr. Tony Armstrong
SAI, Inc.
P. O. Box 2351
La Jolla, CA 92038

Dr. Robert Behringer
ONR
1030 E. Green
Pasadena, CA 91106

Dr. G. Bekefi (5 copies)
Massachusetts Institute of Technology
Bldg. 26
Cambridge, MA 02139

Dr. Arden Bement (2 copies)
Deputy Under Secretary of Defense
for R&AT
Room 3E114, The Pentagon
Washington, D.C. 20301

Dr. T. Berlincourt
Code 420
Office of Naval Research
Arlington, VA 22217

Dr. I. B. Bernstein (2 copies)
Yale University
Mason Laboratory
400 Temple Street
New Haven, CT 06520

Dr. Charles Brau (2 copies)
Applied Photochemistry Division
Los Alamos National Scientic
Laboratory
P. O. Box 1663, M.S. - 817
Los Alamos, NM 87545

Dr. R. Briggs (L-71)
Lawrence Livermore National Lab.
P. O. Box 808
Livermore, CA 94550

Dr. Fred Burskirk
Physics Department
Naval Postgraduate School
Monterey, CA 93940

Dr. K. J. Button
Massachusetts Institute of Technology
Francis Bitter National Magnet Lab.
Cambridge, MA 02139

Dr. Gregory Canavan
Director, Office of Inertial Fusion
U. S. Department of Energy
M.S. C404
Washington, D.C. 20545

Prof. C. D. Cantrell
Center for Quantum Electronics
& Applications
The University of Texas at Dallas
P. O. Box 688
Richardson, TX 75080

Dr. Maria Caponi
TRW, Building R-1, Room 1070
One Space Park
Redondo Beach, CA 90278

Dr. J. Cary
Los Alamos National Scienific
Laboratory
MS 608
Los Alamos, NM 87545

Dr. Weng Chow
Optical Sciences Center
University of Arizona
Tucson, AZ 85721

Dr. Peter Clark
TRW, Building R-1, Room 1096
One Space Park
Redondo Beach, CA 90278

Dr. Robert Clark
P. O. Box 1925
Washington, D.C. 20013

Dr. William Colson
Quantum Institute
Univ. of California at Santa Barbara
Santa Barbara, CA 93106

Dr. William Condell
Code 421
Office of Naval Research
Arlington, VA 22217

Dr. Richard Cooper
Los Alamos National Scientific
Laboratory
P. O. Box 1663
Los Alamos, NM 87545

Cmdr. Robert Cronin
NFOIO Detachment, Suitland
4301 Suitland Road
Washington, D.C. 20390

Dr. R. Davidson (5 copies)
Plasma Fusion Center
Massachusetts Institute of Technology
Cambridge, MA 02139

Dr. John Dawson (2 copies)
Physics Department
University of California
Los Angeles, CA 90024

Dr. David Deacon
Physics Department
Stanford University
Stanford, CA 94305

Defense Technical Information Center (12 copies)
Cameron Station
5010 Duke Street
Alexandria, VA 22313

Dr. Francesco De Martini
Instituto de Fiscia
G. Marconi" Univ.
Piazzo delle Science, 5
ROMA00185 ITALY

Prof. P. Diament
Columbia University
Dept. of Electrical Engineering
New York, NY 10027

Prof. J. J. Doucet (5 copies)
Ecole Polytechnique
91128 Palaiseau
Paris, France

Dr. John Elgin (2 copies)
Imperial College
Dept. of Physics (Optics)
London SWF, England

Dr. Luis R. Elias (2 copies)
Quantum Institute
University of California
Santa Barbara, CA 93106

Dr. David D. Elliott
SRI International
33 Ravenswood Avenue
Menlo Park, CA 94025

Dr. Jim Elliot (2 copies)
X-Division, M.S. 531
Los Alamos National Scientific Laboratory
Los Alamos, NM 87545

Director (2 copies)
National Security Agency
Fort Meade, MD 20755
ATTN: Mr. Richard Foss, A42

Dr. Robert Fossum, Director
DARPA
1400 Wilson Boulevard
Arlington, VA 22209 (2 copies)

Dr. Edward A. Frieman
Director, Office of Energy Research
U. S. Department of Energy
M.S. 6E084
Washington, D.C. 20585

Dr. George Gamota (3 copies)
OUSDRE (R&AT)
Room 3D1067, The Pentagon
Washington, D.C. 20301

Dr. Richard L. Garwin
IBM, T. J. Watson Research Center
P. O. Box 218
Yorktown Heights, NY 10598

Dr. Edward T. Gerry, President
W. J. Schafer Associates, Inc.
1901 N. Fort Myer Drive
Arlington, VA 22209

Dr. Avraham Gover
Tel Aviv University
Fac. of Engineering
Tel Aviv, ISRAEL

Mr. Donald L. Haas, Director
DARPA/STO
1400 Wilson Boulevard
Arlington, VA 22209

Dr. P. Hammerling
La Jolla Institute
P. O. Box 1434
La Jolla, CA 92038

Director
National Security Agency
Fort Meade, MD 20755
ATTN: Mr. Thomas Handel, A243

Dr. William Happer
560 Riverside Drive
New York City, NY 10027

Dr. Robert J. Hermann
Assistant Secretary of the
Air Force (RD&L)
Room 4E856, The Pentagon
Washington, D.C. 20330

Dr. Rod Hiddleston
KMS Fusion
Ann Arbor, MI 48106

Dr. J. L. Hirshfield (2 copies)
Yale University
Mason Laboratory
400 Temple Street
New Haven, CT 06520

Dr. R. Hofland
Aerospace Corp.
P. O. Box 92957
Los Angeles, CA 90009

Dr. Fred Hopf
University of Arizona
Tucson, AZ 85721

Dr. Benjamin Huberman
Associate Director, OSTP
Room 476, Old Executive Office Bldg.
Washington, D.C. 20506

Dr. S. F. Jacobs
Optical Sciences Center
University of Arizona
Tucson, AZ 85721

Dr. S. Johnston
Dept of Electrical Engineering
Columbia University
N.Y., N.Y. 10027

Mr. Eugene Kopf
Principal Deputy Assistant
Secretary of the Air Force (RD&L)
Room 4E964, The Pentagon
Washington, D.C. 20330

Prof. N. M Kroll
La Jolla Institutes
P. O. Box 1434
La Jolla, CA 92038

Dr. Tom Kuper
Optical Sciences Center
University of Arizona
Tucson, AZ 85721

Dr. Thomas Kwan
Los Alamos National Scientific
Laboratory
MS608
Los Alamos, NM 87545

Dr. Willis Lamb
Optical Sciences Center
University of Arizona
Tucson, AZ 85721

Mr. Mike Lavan
BMDATC-O
ATTN: ATC-O
P. O. Box 1500
Huntsville, AL 35807

Dr. John D. Lawson (2 copies)
Rutherford High Energy Lab.
Chilton
Didcot, Oxon OX11 OOX
ENGLAND

Mr. Ray Leadabrand
SRI International
333 Ravenswood Avenue
Menlo Park, CA 94025

Mr. Barry Leven
NISC/Code 20
4301 Suitland Road
Washington, D.C. 20390

Dr. Donald M. LeVine (3 copies)
SRI International
1611 N. Kent Street
Arlington, VA 22209

Dr. Anthony T. Lin
University of California
Los Angeles, CA 90024

Director (2 copies)
National Security Agency
Fort Meade, MD 20755
ATTN: Mr. Robert Madden, R/SA

Dr. John Madey
Physics Department
Stanford University
Stanford, CA 94305

Dr. Joseph Mangano
DARPA
1400 Wilson Boulevard
Arlington, VA 22209

Dr. S. A. Mani
W. J. Schafer Associates, Inc.
10 Lakeside Office Park
Wakefield, MA 01880

Dr. Mike Mann
Hughes Aircraft Co.
Laser Systems Division
Culver City, CA 90230

Dr. T. C. Marshall
Applied Physics Department
Columbia University
New York, NY 10027

Mr. John Meson
DARPA
1400 Wilson Boulevard
Arlington, VA 22209

Dr. Pierre Meystre
Projektgruppe fur Laserforschung
Max Planck Gesellschaft
Garching, MUNICH WEST GERMANY

Dr. Gerald T. Moore
Optical Sciences Center
University of Arizona
Tucson, Az 85721

Dr. Philip Morton
Stanford Linear Accelerator Center
P. O. Box 4349
Stanford, CA 94305

Dr. Jesper Munch
TRW
One Space Park
Redondo Beach, CA 90278

Dr. George Neil
TRW
One Space Park
Redondo Beach, CA 90278

Dr. Kelvin Neil
Lawrence Livermore National Lab.
Code L-321, P. O. Box 808
Livermore, CA 94550

Dr. Brian Newnam
MS 564
Los Alamos National Scientific
Laboratory
P. O. Box 1663
Los Alamos, NM 87545

Dr. Milton L. Noble (2 copies)
General Electric Company
G. E. Electric Park
Syracuse, NY 13201

Prof. E. Ott (2 copies)
University of Maryland
Dept. of Physics
College Park, MD 20742

Dr. Richard H. Pantell
Stanford University
Stanford, CA 94305

Dr. Claudio Parazzoli
Highes Aircraft Company
Building 6, MS/C-129
Centinela & Teale Streets
Culver City, CA 90230

Dr. Richard M. Patrick
AVCO Everett Research Lab., Inc.
2385 Revere Beach Parkway
Everett, MA 02149

Dr. Claudio Pellegrini
Brookhaven National Laboratory
Associated Universities, Inc.
Upton, L.I., NY 11973

The Honorable William Perry
Under Secretary of Defense (R&E)
Office of the Secretary of Defense
Room 3E1006, The Pentagon
Washington, D.C. 20301

Dr. Alan Pike
DARPA/STO
1400 Wilson Boulevard
Arlington, VA 22209

Dr. Hersch Pilloff
Code 421
Office of Naval Research
Arlington, VA 22217

Dr. Charles Planner
Rutherford High Energy Lab.
Chilton
Didcot, Oxon, OX11, 00X
ENGLAND

Dr. Michal Poole
Daresbury Nuclear Physics Lab.
Daresbury, Warrington
Cheshire WA4 4AD
ENGLAND

Dr. Don Prosnitz
Lawrence Livermore National Lab.
Livermore, CA 94550

Dr. D. A. Reilly
AVCO Everett Research Lab.
Everett, MA 02149

Dr. James P. Reilly
W. J. Schafer Associates, Inc.
10 Lakeside Office Park
Wakefield, MA 01880

Dr. A. Renieri
C.N.E.N.
Div. Nuove Attivita
Dentro di Frascatti
Frascatti, Rome
ITALY

Dr. Daniel N. Rogovin
SAI
P. O. Box 2351
La Jolla, CA 92038

Dr. Michael Rosenbluh
MIT - Magnet Laboratory
Cambridge, MA 02139

Dr. Marshall N. Rosenbluth
Institute for Advanced Study
Princeton, NJ 08540

Dr. Eugene Ruane (2 copies)
P. O. Box 1925
Washington, D.C. 20013

Dr. Antonio Sanchez
MIT/Lincoln Laboratory
Room B231
P. O. Box 73
Lexington, MA 02173

Dr. Aleksandr N. Sandalov
Department of Physics
Moscow University
MGU, Lenin Hills
Moscow, 117234, USSR

Prof. S. P. Schlesinger
Columbia University
Dept. of Electrical Engineering
New York, NY 10027

Dr. Howard Schlossberg
AFOSR
Bolling AFB
Washington, D.C. 20332

Dr. Stanley Schneider
Rotodyne Corporation
26628 Fond Du Lac Road
Palos Verdes Peninsula, CA 90274

Dr. Marlan O. Scully
Optical Science Center
University of Arizona
Tucson, AZ 85721

Dr. Steven Segel
KMS Fusion
3621 S. State Street
P. O. Box 1567
Ann Arbor, MI 48106

Dr. Robert Sepucha
DARPA/STO
1400 Wilson Boulevard
Arlington, VA 22209

Dr. A. M. Sessler
Lawrence Berkeley Laboratory
University of California
1 Cyclotron Road
Berkeley, CA 94720

Dr. Earl D. Shaw
Bell Labs
600 Mountain Avenue
Murray Hill, NJ 07974

Dr. R. Shefer
Massachussetts Institute of
Technology
Bldg. 26
Cambridge, MA 02139

Dr. Chan-Chin Shih
R&D Associates
P. O. Box 9695
Marina Del Rey, CA 92091

Dr. Jack Slater
Mathematical Sciences, NW
P. O. Box 1887
Bellevue, WA 98009

Dr. Kenneth Smith
Physical Dynamics, Inc.
P. O. Box 556
La Jolla, CA 92038

Mr. Todd Smith
Hansen Labs
Stanford University
Stanford, CA 94305

Dr. Joel A. Snow
Senior Technical Advisor
Office of Energy Research
U. S. Department of Energy, M.S. E084
Washington, D.C. 20585

Dr. Richard Spitzer
Stanford Linear Accelerator Center
P. O. Box 4347
Stanford, CA 94305

Mrs. Alma Spring
DARPA/Administration
1400 Wilson Boulevard
Arlington, VA 22209

DRI/MP Reports Area G037 (2 copies)
333 Ravenswood Avenue
Menlo Park, CA 94025
ATTN: D. Leitner

Dr. Abraham Szoke
Lawrence Livermore National Lab.
MS/L-470, P. O. Box 808
Livermore, CA 94550

Dr. Milan Tekula
AVCO Everett Research Lab.
2385 Revere Beach Parkway
Everett, MA 02149

Dr. John E. Walsh
Department of Physics
Dartmouth College
Hanover, NH 03755

Dr. Wasneski (2 copies)
Naval Air Systems Command
Department of the Navy
Washington, D.C. 20350

Ms. Bettie Wilcox
Lawrence Livermore National Lab.
ATTN: Tech. Info. Dept. L-3
P. O. Box 808
Livermore, CA 94550

Dr. A. Yariv
California Institute of Tech.
Pasadena, CA 91125